Laser ablation ICP-MS in paleoceanography: A regional study on the benthic foraminifer *Oridorsalis umbonatus* in the Benguela Upwelling Area off Namibia

Dissertation zur Erlangung des Doktorgrades der Naturwissenschaften

am Fachbereich Geowissenschaften
der Universität Bremen

vorgelegt von

Söhnke Rathmann

Bremen, August 2008

Tag des Kolloquiums:
12. Dezember 2008

Gutachter:
Prof. Dr. Gerold Wefer
Prof. Dr. Andreas Mackensen

Prüfer:
PD Dr. Matthias Zabel
Prof. Dr. Tilo von Dobeneck

Danksagung

Für die Vergabe der Arbeit und die Betreuung möchte ich mich ganz herzlich bei Prof. Dr. Gerold Wefer bedanken. Mein gleichfalls besonderer Dank geht an Dr. Stefan Mulitza, der mir immer mit Unterstützung, Ideen und zur Diskussionen zur Seite stand und die Arbeit dadurch entscheidend weiter brachte. Für die freundliche Übernahme des Zweitgutachtens gilt mein Dank Prof. Dr. Andreas Mackensen.

Dr. Henning Kuhnert danke ich dafür, mir die Geheimnisse des Laser ablation Systems und des Massenspektrometers näher gebracht zu haben um so den Foraminiferen ihre Geheimnisse zu entlocken.

Desweiteren gilt mein Dank Kapitän und Crew auf FS METEOR auf der Reise M57/2 sowie den Kolleginnen und Kollegen, im besonderen denen aus dem Geolabor, an Bord. Es war eine schöne und erfolgreiche Zeit mit Euch an Bord!

Weiterhin gilt mein Dank all jenen Kolleginnen und Kollegen aus dem Fachbereich, die für das tolle Arbeitsklima gesorgt haben und immer zu Diskussionen bereit waren. Vor allem waren dies Oscar Romero, Barbara Donner, André Paul, Harald Paulsen, Ismene Seeberg-Elverfeldt und Snježana Žarić. Die beiden letztgenannten sowie meine Zimmergenossin Iris Wilke sorgten mit Ihren Computerproblemen auch gerne für kürzere Ablenkungen. Nach der Lösung der Problemchen (meistens war es ja nicht mehr) konnte ich mich wieder mit frischem Elan in die eigentliche Arbeit stürzen! Weiterhin danke ich Iris Wilke und Rik Tjallingii die sich das Büro mit mir geteilt haben. Es gab immer nette Diskussionen mit Euch, auch wenn sie nicht alle fachlich waren.

Für die Unterstütung bei den analytischen Untersuchungen danke ich Dr. Barbara Donner und Dr. Sylvia Hess, die mir die planktischen und benthischen Foraminiferen näher gebracht habe, Dr. Oscar Romero der mich in den XRF-Scanner eingewiesen und mit mir zusammen die Kerne von M57/2 gemessen hat, sowie Dr. Monika Segl und Ihr Team für die Messung der stabilen Isotopen.

Meiner Frau Cessna und meiner Familie danke ich dafür, daß sie mich immer unterstützt haben, vor allem, wenn es mit der Arbeit mal nicht so gut lief. Ihr habt mir immer wieder die nötige Kraft und Energie gegeben diese Arbeit zu verwirklichen, auch wenn es dann doch etwas länger gedauert hat, sie zum Abschluß zu bringen!

Für die letzten Korrekturen und den „Feinschliff“ möchte ich mich neben den Co-Autoren der Artikel (Kapitel 2–4) besonders bei Iris und Snježana bedanken, die bereit waren meine Einleitung und das Schlußwort mit hilfreichen Hinweisen zu versehen!

Diese Arbeit wurde von der Deutschen Forschungsgemeinschaft im Rahmen des Forschungszentrums Ozeanränder finanziell unterstützt.

Table of Contents

Abstract

The different benthic foraminiferal species (epibenthic as well as endobenthic) colonize wide areas of the ocean floor and are widely used for paleoceanographic reconstructions. To improve these reconstructions, it is an important part in research to continuously develop and refine proxies by e.g. improving measuring techniques as well as introducing other species in paleoceanograhpy. The main focus of the presented thesis is a regional examination of the trace element ratios of the rarely used benthic foraminifer *Oridorsalis umbonatus* and the investigation of their suitability for paleoceanographic applications. Since *O. umbonatus* is not very abundant in the sediments, it was necessary – as a prerequisite for such studies – to investigate, whether laser ablation ICP-MS can be used for trace element measurements on benthic foraminifera.

Therefore, as a first step, trace elements were measured using laser ablation ICP-MS on a set of modern core top samples collected along a depth transect on the continental slope off Namibia at $25.5°$S ($320 - 2300$m water depth; $2.9°$ to $10.4°$C). The Mg/Ca ratios where than calibrated against bottom water temperatures (BWT). The study demonstrates clearly that benthic foraminiferal trace elements can be reliably measured with the laser ablation technique and that the Mg/Ca ratio of *O. umbonatus* has the potential to be used as a proxy for BWTs. The resulting Mg/Ca–BWT relationship of *O. umbonatus* is described by the exponential equation $\mathrm{Mg/Ca} = 1.528 * e^{0.09 * \mathrm{BWT}}$. The temperature sensitivity of this equation is similar to previously published calibrations based on *Cibicidoides* species suggesting that the Mg/Ca ratio of *O. umbonatus* is a valuable proxy for thermocline and deep water temperatures.

For the last few years the influence of the carbonate ion concentration ($[CO_3^{2-}]$) on the trace element and stable isotope incorporation in calcareous shells has been intensely discussed. Hence, the dependency on trace elements and stable isotopes in the tests of *O. umbonatus* was analysed as a second step. Modern core top samples from the Namibian continental slope suggest that the shell composition of this species is influenced by the chemistry of the pore-water. However, for these organic-rich sediments, the impact of ocean bottom water properties on both pore-water and shell chemistry is surprisingly small. Sr/Ca correlates negatively with $[CO_3^{2-}]$ and to a lesser extent to $\Delta[CO_3^{2-}]$, which is opposed to previous results. A correlation between shell $\delta^{18}O$ (corrected for temperature and $\delta^{18}O_{seawater}$) and $[CO_3^{2-}]$ was found, however, the variability of the corrected $\delta^{18}O$ is close to the analytical limit. No clear dependences were observed for $\delta^{13}C$ and Mg/Ca on $[CO_3^{2-}]$.

In a third step, the above findings were used to investigate the changes in the water mass stratification off Namibia between the Holocene and the Last Glacial Maximum (LGM). Trace elements and stable isotopes of *O. umbonatus* were measured on six multicores and six gravity cores to determine BWTs and salinity. The calculated sea water density reveals that our samples follow the water masses downslope in the regular sequence. BWTs show nearly no changes between LGM and modern values. Interestingly, in the shallow cores, which were most influenced by LGM conditions,

we even observe slightly warmer BWTs during the LGM, which are in contrast to the findings of Niebler et al. (2003), who investigated inter alia nearby cores with a modified version of the Imbrie-Kipp-Tranfer-Function to reconstruct sea surface temperatures. This contrary changes in the sea surface and bottom water temperatures suggest a shift in the water masses during the LGM.

1. Introduction

1.1. Motivation and scientific objectives

In the field of paleoceanography scientists investigate the climate of the past. The knowledge about ancient natural climatic variations is important to understand how the climate system will react to changes, e.g. the raise of the atmospheric CO_2-concentration. Because it is not possible to measure ancient environmental conditions directly, we have to use measurable replacement indicators for e.g. the temperature. These replacement indicators are called proxies. Proxies make it possible to reconstruct past climatic conditions and are useful to validate paleoceanographic models, which in turn can be used for climate predictions (e.g. Houghton et al., 1995; Fischer and Wefer, 1999; Houghton et al., 2001, and references therein).

In general, proxies are calibrated using a modern reference dataset that includes a range of both corresponding values, the one of the proxy and the one of the respective target parameter. If their relationship is understood, the proxy can be applied to the sedimentary record for paleoceanographic reconstructions. Various constituents of the fauna and flora are used in paleoceanography. An excellent overview about the state of the art of the different proxies is given in Wefer et al. (1999).

The most used proxies to reconstruct water temperatures are alkenones, foraminiferal assemblages, oxygen isotopes, coralline Sr/Ca ratios and foraminiferal Mg/Ca ratios, but there remains significant disagreement (up to $5°C$ and up to 2000 years) between the temperatures reconstructed by these various proxies (Lea et al., 2000; Mollenhauer et al., 2005). Therefore it is crucial to understand the controls of different palaeotemperature proxies and to continuously refine them as well as develop new proxies to ensure that we can accurately reconstruct the past.

Planktic and benthic foraminifera are widely distributed throughout the world's oceans and are major carbonate producers, which accounts for their high fossilization potential. Therefore, foraminifera have been used for the reconstruction of paleoenvironmental parameters for many years (e.g. McCrea, 1950; Emiliani, 1955). In this context not only the proxy itself, but also the chosen measuring technique can play an important role. Boyle and Keigwin (1985) were among the first, who used a liquid solution of foraminiferal shells to measure trace elements, and established a cleaning method, which even today is the basis for trace element measurements with liquid solution on foraminiferal tests. However, not only is this cleaning procedure very extensive, the liquid solution method also needs a certain amount of sample material. Yet there are other methods to measure trace elements as well, like e.g. Laser Ablation Inductively Coupled Plasma Mass Spectrometry (LA-ICP-MS). This method is fast and reliable and needs less material in the process than the liquid solution method. In addition, the sample material is reusable for further investigations such as stable isotope measurements. A further benefit is the possibility to omit the time consuming

cleaning method.

Oridorsalis umbonatus is a benthic foraminiferal species that covers a broad depth range ($320 - 4000$m water depth) as well as a wide time span since the Tertiary. These broad temporal and spatial ranges make *O. umbonatus* an interesting species for further investigations. However, due to the often very limited number of tests being found in the sediment, so far there have been only few investigations on this species world wide. Moreover, as stated above, dependencies between proxies and target parameters are mostly calibrated with world wide reference datasets. However, especially for benthic foraminifera, regional calibrations may be more effective and reasonable because they consider the specific regional circumstances that have more influence on benthic species than on planktic foraminifera, which are more mobile. E.g. Lear et al. (2002) made a global calibration for a Mg/Ca-temperature relationship of *O. umbonatus*, but they found only a weak regression ($R^2 = 0.4$). A regional regression for this species was never made, because mostly other species like *Cibicidoides wuellerstorfi* take precedence over *O. umbonatus* due to their higher frequency of occurence in the region. Only through the introduction of the laser ablation method, which is able to produce reliable results from significantly smaller amounts of sample material, this species is now brought to the spotlight. Therefore, a regional calibration between its trace element ratios and bottom water temperatures (BWT) using the new promising method of laser ablation should be the first step to explore its potential in paleoceanography.

Based on the above considerations, the scientific objectives for this study were

- to test if laser ablation is applicable to measure trace elements on *O. umbonatus*,
- to calibrate the trace element ratios of *O. umbonatus* with the BWT for a specific region (Benguela Upwelling System) and to compare the resulting calibration with other calibrations from the literature either on the same species (Lear et al., 2002) or on other benthic species in a comparable temperature range (Rosenthal et al., 1997),
- to investigate whether there is an influence of carbonate ion concentration ($[CO_3^{2-}]$) and carbonate ion saturation ($\Delta[CO_3^{2-}]$) on Mg/Ca, Sr/Ca and stable isotopes as discovered previously (e.g. Russell and Spero, 2000; Boyle and Erez, 2003; Russell et al., 2004; Elderfield et al., 2006) and to quantify this potential influence on the related parameters,
- to paleoceanographically apply the calibration on a timeslice from the sedimentary record (Last Glacial Maximum, LGM), and
- to compare our results for the BWT with the findings of Niebler et al. (2003), who investigated sea surface temperatures (SST) of the LGM in the same region, which were up to $10°C$ lower than today.

1.2. Trace elements

The analysis of a wide range of trace elements, like Cd, Ba, Mg, Sr and U to name the most commonly used, has been applied in paleoceanography since the mid of the

last century. After it was used first on magmatic rocks, it became more and more important on calcareous shells. Temperature dependencies of Mg/Ca and Sr/Ca ratios are known since more than three decades (Oomori et al., 1987; Katz, 1973). The first investigations to determine the relationship between the trace element incorporation and the temperature have been done on corals (Harriss and Almy, 1964). Besides corals, trace elements are used from the calcareous shells of ostracodes (Müller, 2000; Morishita et al., 2007), foraminifera and, less frequently, bivalves (Epplé, 2004) and otoliths of salmon (Arai et al., 2006). Most common is the temperature dependency of the Sr/Ca ratio (if Sr/Ca is higher than 5 mmol/mol as e.g. in corals) or the Mg/Ca ratio (if Sr/Ca is lower than 5 mmol/mol as e.g. in foraminifera) (see Müller, 2000).

Because of the low concentrations of trace elements in the shells, the usefulness of trace element proxies was limited by the low accuracy of the measuring techniques for a long time. Significantly improved measurements, that are possible since just more than a decade, now make this method a promising technique, which is able to provide quantitative information about past climates. Mg/Ca ratios in foraminiferal calcite are one of the most applied of these palaeotemperature proxies, and are used to assess past SST (Barker et al., 2005) and BWTs (Lear et al., 2000) from planktic and benthic foraminifera, respectively. A powerful advantage in using the Mg/Ca palaeotemperature proxy is the possibility to reconstruct the sea salinity if used together with the foraminiferal calcite $\delta^{18}O$ record, assuming the relationship between salinity and $\delta^{18}O$ seawater is known (Wolff et al., 1999).

The Mg/Ca ratios in modern planktic foraminifera have been demonstrated to be primarily a function of the temperature and the Mg/Ca ratio of the water in which they grew (Nürnberg et al., 1996; Lea et al., 2000; Elderfield and Ganssen, 2000; Dekens et al., 2002; Anand et al., 2003; Barker et al., 2005). The Mg/Ca ratio in seawater is spatially constant and changes on timescales of less than 1 million years due to the very long residence times of both Mg and Ca in the oceans (Broecker and Peng, 1982), but individual measurements show significant scatter around calibrations of the Mg/Ca palaeothermometer (Elderfield and Ganssen, 2000; Anand et al., 2003). Furthermore, there are notable differences between the various existing calibrations derived from different ocean regions (e.g. for *Globigerinoides ruber* (white), Elderfield and Ganssen, 2000; Lear et al., 2002). Therefore, regional calibrations seem to be appropriate.

The degree of scatter limits the precision of Mg/Ca as a palaeotemperature proxy and calls the accuracy of the technique into question. An unsuccessful attempt to advance this method was conducted by Wu and Hillaire-Marcel (1995), who used laser ablation instead of liquid solution on benthic foraminiferal tests. This new measuring technique was successful only after the development of new laser ablation systems with a higher accuracy, which were applied on planktic foraminifera for the first time (Eggins et al., 2003; Reichart et al., 2003). Since this technique allows to measure several tests per sediment sample and even to make multiple measurements per test, it is possible to balance some scattering by excluding data off a 2σ level when calculating the mean for that sample. However it is likely, that there are additional oceanographic variables that affect the incorporation of Mg into foraminiferal calcite. Laboratory culture studies have shown that the carbonate ion concentration has an effect on Mg/Ca ratios in foraminifera but suggest that its influence is small in comparison with temperature (Lea, 1999; Nürnberg et al., 1996; Russell et al., 2004; Elderfield et al., 2006).

In benthic foraminifera, increased Mg/Ca ratios have been observed to correlate with increased carbonate ion concentrations (Elderfield et al., 2006; Boyle and Erez, 2003). In contrast, a laboratory study of planktic foraminifera (Russell et al., 2004), showed decreasing Mg/Ca ratios with increasing carbonate ion concentrations.

1.3. Working area

The working area is located off the coast of Namibia around $25°$S within the Benguela Upwelling System. The Benguela high-productivity system is situated off Southwest Africa adjacent to the coasts of Namibia and South Africa (Figure 1.1). Its northern and southern boundaries are defined as the Angola-Benguela frontal zone and the Agulhas retroflection, respectively. The northern boundary is formed by the Walvis Ridge which at about $19.5°$S is connected with the continental shelf via a shallow sill (< 2500m), that is referred to as Walvis Plateau.

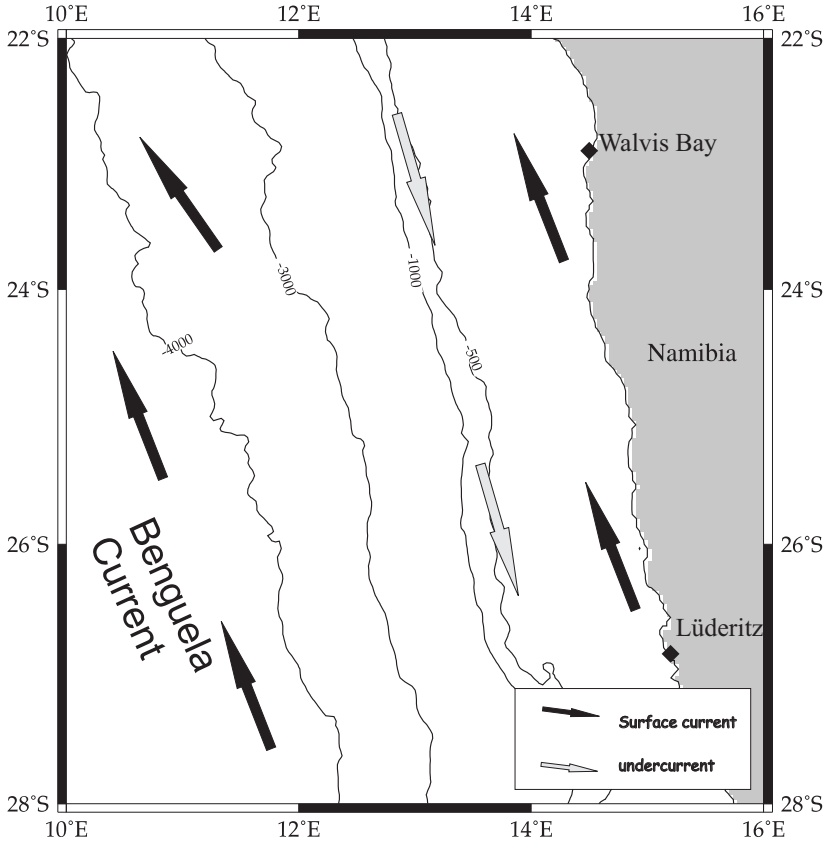

Figure 1.1.: Overview map of the working area, including the main currents (black: surface currents, grey: undercurrents).

The shelf width and depth in the Cape Basin are variable. Double shelf breaks are common, in particular near Walvis Bay ($23°$S, see Figure 1.2). The outer shelf is relatively deep in large areas with the major shelf break at a water depth of about 400m. The SE trade winds are prevailing in the Benguela area, as described in detail by Shannon and Nelson (1996). Upwelling favourable winds are perennial in the northern part of the system, while in the South, distinct upwelling maxima occur in

spring and summer. Consequently, the upwelling system is commonly divided into a northern part with perennial upwelling and a southern half with stronger seasonality. The border between the two subsystems is usually drawn near Lüderitz at 27°S. In this study, we focus on the northern part near the border of the two subsystems.

The prevailing southeasterly trade winds drive coastal upwelling of cold and nutrient-rich waters originating from depths of 200−300m in the body of the South Atlantic Central Water (Shannon, 1985). Upwelling of these nutrient-rich water masses leads to high productivity resulting in high concentrations of chlorophyll-a in surface waters (Figure 1.3a) and low SST (Figure1.3b). Upwelling in the Benguela system occurs in a number of distinct upwelling cells, which form at locations of maximum wind

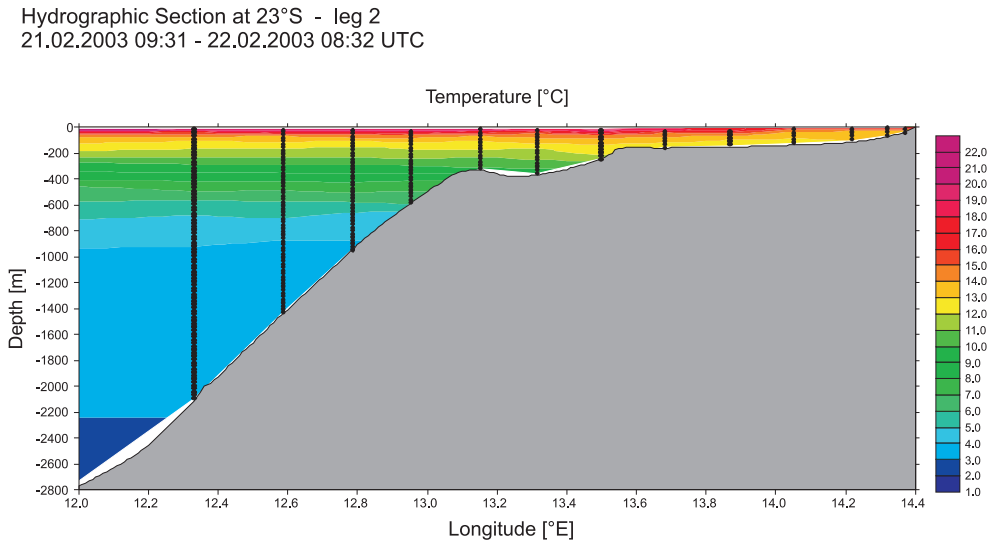

Figure 1.2.: Temperature section off Walvis Bay (Moorholz and Heene, 2003a). Black vertical lines indicate CTD-measurements.

stress curl and where there is a change in orientation of the coastline (Lutjeharms and Meeuwis, 1987; Shannon and Nelson, 1996). Upwelling events are strongest, most frequent, and extend furthest offshore at the Lüderitz cell centered at 27°S (see Figure 1.3). Productivity is also high on the Walvis Plateau (near 19°S) and near Walvis Bay (22°S) (Lutjeharms and Meeuwis, 1987; Summerhayes et al., 1995). However, there is some disagreement between different authors whether the high productivity at Walvis Bay results from upwelling as stated by Lutjeharms and Meeuwis (1987) or whether the physical requirements for upwelling, such as wind stress, are not given in the area (Shannon, 1985). Between 18°S and 34°S, a longshore thermal front coincident with the shelf break demarcates the seaward extent of the upwelled water. This front is highly convoluted and often disturbed by filaments and eddies, sometimes extending as far as 1300km offshore (Summerhayes et al., 1995). On the offshore side of the front, secondary upwelling may occur. It has been noted that enhanced phytoplankton productivity often occurs not in the center of upwelling cells, but rather offshore and at the borders of or just outside upwelling sites (Lutjeharms and Stockton, 1987, and references therein). Therefore the development of an extensive and highly convoluted field of filaments, eddies and thermal fronts, as can be found offshore Lüderitz, is favorable for high productivity.

A poleward undercurrent has been reported for the shelf and the upper slope off Namibia (Shannon and Nelson, 1996) and can be modeled to follow the shelf break using a time-dependent, wind- and density-driven physical model (Fennel, 1999; Skogen, 1999). The structure of the shelf and slope and the temperature distribution are shown in Figure 1.2. Upwelling will occur on the shelf break ($\sim$ 13°E) and on the shelf $\sim$ 1.5° closer to the coast. Occasional bergwinds perpendicular to the coast

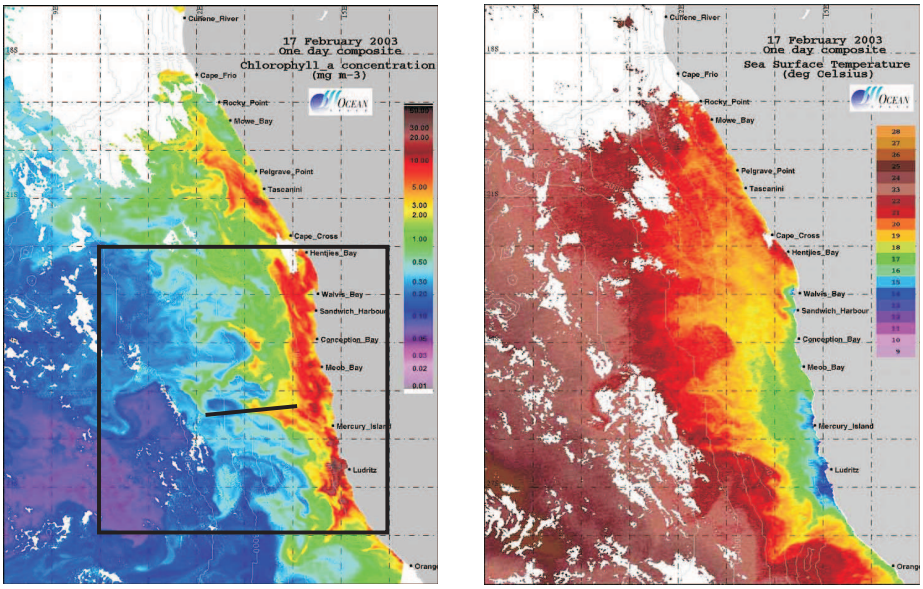

(a) Chlorophyll-a (b) SST

Figure 1.3.: Chlorophyll-a (a) and SST (b) maps with SeaWIFS data. The black box in the left figure denotes the working area, the black line the transect.

are the dominant means of transport for terrestrial material in the prevailing arid climate. However, only insignificant relative contributions of terrigenous particles to total fluxes were observed in sediment traps (Wefer and Fischer, 1993; Giraudeau et al., 2000). Terrestrial input, in particular terrestrial input of organic matter, can therefore be considered to be of minor importance in the area, which is also confirmed by the stable organic carbon isotope composition ($\delta^{13}C_{org}$) exhibiting consistently marine values in surface sediments (Fischer et al., 1998).

Off Namibia, the surface layer is characterized by warm water of higher salinity originating from the northern Benguela area. The SST increases offshore, whereas at the coast a very weak upwelling structure is found. Below the surface mixed layer the thermocline water off Namibia consists of two different central water masses and their mixing stages. Saline, nutrient rich but oxygen depleted South Atlantic Central water (SACW) originating from the tropical ecosystem enters the Benguela system from the north covering the entire shelf and the continental margin to 12.2°E. Fresher, nutrient-depleted and oxygen-rich Eastern South Atlantic Central Water (ESACW) is transported with the Benguela Current (BC) northward. The distribution of both central water types is shown in Figure 1.4. In the upper central water layer (13°C isotherm, $\sim$ 150m depth) the SACW extends down to 24°S and covers only the shelf. The major portion of the upwelled water at the coast is originating from this depth. This causes a higher on shore transport of central water. In the deeper layers the

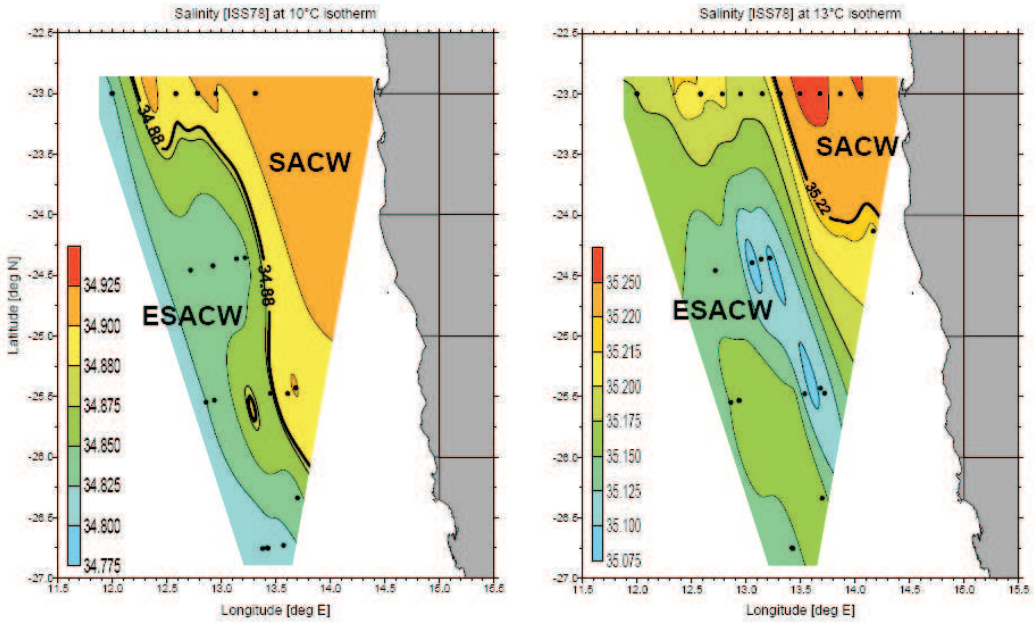

Figure 1.4.: Horizontal distribution of salinity at the 10°C isotherm (left) and at the 13°C isotherm (right) off the Namibian coast. The front between the two central water types is depicted by the bold isoline. (Moorholz and Heene, 2003b)

southward extension of SACW at the shelf increases (see salinity distribution at the 10°C isotherm, $\sim$ 250m depth). This may be caused by a higher intensity of the poleward undercurrent and a decreasing shore ward transport of ESACW. Due to their different oxygen and nutrient contents the distribution of central water masses plays an important role for the ventilation of the subsurface layer and the productivity of the Benguela Upwelling System (Moorholz and Heene, 2003b).

The central water masses are underlain by the Antarctic Intermediate Water (AAIW). The core of the AAIW can be identified using the salinity minimum at 800m depth as an indicator. The secondary salinity maximum close to 2200m is associated with the North Atlantic Deep Water (NADW).

1.4. Material and Methods

The Department of Geosciences at Bremen University, especially the Sonderforschungsbereich (SFB) 261 “The South Atlantic in the Late Quaternary – Reconstruction of Material Budgets and Current Systems”, had a research focus on the upwelling area off Namibia since 1989, and a broad set of samples was collected and investigated. The aim of the SFB was the application and development of proxies for the reconstruction of current and productivity systems in the region over the last $300,000$ years. These extensive investigations make this area an ideal field to test new measuring techniques and proxies from formerly less used species because of the broad range of published results to compare and validate the own findings with.

1.4.1. Sample material

On the R/V METEOR cruises M34/1, M34/2 and M57/2 (Bleil and cruise participants, 1996; Schulz and cruise participants, 1996; Zabel and cruise participants, 2003), multicores and gravity cores were collected on the shelf and the slope off Namibia between Walvis Bay in the north and Lüderitz in the south from $50 - 3000$m water depth (Figure 1.5). Bottom water temperatures were measured with a conductivity-temperature-depth logger (CTD SBE 911+) (Moorholz and Heene, 2003a) on each multicorer position on cruise M57/2.

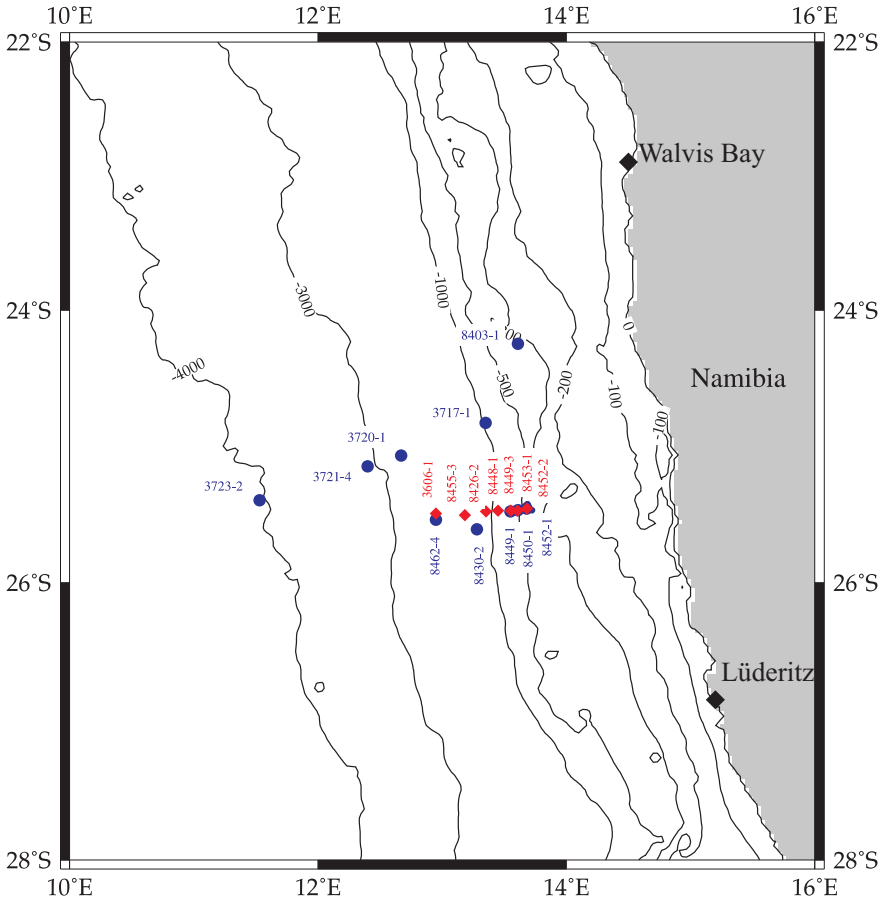

Figure 1.5.: Core locations of the multicores and gravity cores off Namibia from M34/1, M34/2 and M57/2 (Bleil and cruise participants, 1996; Schulz and cruise participants, 1996; Zabel and cruise participants, 2003). Red diamonds: gravity cores; blue circles: multicores.

On board of R/V METEOR the sediments (mostly nannofossil ooze) were cut into 1cm slices immediately upon recovery and were preserved and stained with an ethanol/Rose Bengal solution, which stains only living cells. The multicores from M57/2 (Zabel and cruise participants, 2003) were used to calibrate the Mg/Ca-temperature-relationship for the endobenthic foraminiferal species *O. umbonatus*. The same multicores and additional ones from M34/2 (Schulz and cruise participants, 1996) were used to improve the calibration and for further analyses on trace elements and stable isotopes.

For the paleoceanographic application of the new proxy, gravity cores from M57/2 (Zabel and cruise participants, 2003) and gravity core GeoB3606-1 from M34/1 (Bleil and cruise participants, 1996) were used. Gravity corer with pipe lengths of either 6, 12 or 18m, and a weight of 2.5 tons were deployed (see red diamonds in Figure 1.5). In order to retain the relative orientation of the cores, all liners used had been marked

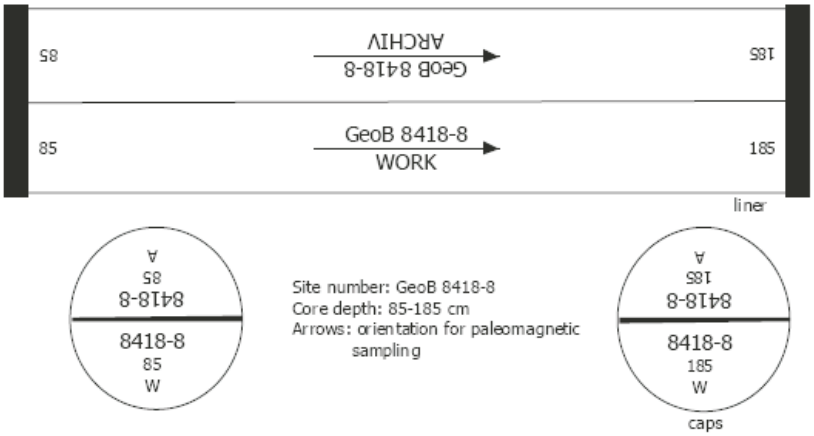

Figure 1.6.: Scheme of the inscription of gravity core segments.

lengthwise with a straight line. On board, the sediment cores were cut into 1−meter sections, closed up with caps on both ends and labeled according to a standard scheme (Figure 1.6). Core segments were cut into "archive" and "work" halves. The "archive" half was used for core description, smear slide sampling, core photography, and scanning of light reflectance. For geochemical and foraminiferal analyses the "work" half was sampled with two series of 10−ml syringes at 5cm intervals.

1.4.2. Sample preparation

Multicores After the initial preparation on board as described in Section 1.4.1 the samples were washed over a 125μm and a 63μm sieve and were dried at 50°C at the laboratory in Bremen. A binocular microscope was used to collect five to ten individuals of *O. umbonatus* with a diameter of $300 - 400\mu$m out of the topmost cm of each sample. Only well preserved tests (with all chambers) were used. In all samples, Rose Bengal stained shells were present, which indicates modern sediments.

The CTD-measured BWTs derived on cruise M57/2 fall well within the seasonal temperature range derived from the World Ocean Atlas (WOA) (Levitus and Boyer, 1994; Stephens et al., 2002) for the coring sites. The BWTs at the investigated sites cover a range from 2.9° to 10.4°C. Since there are no CTD-data available for the multicorer positions from cruise M34/2, BWTs from the WOA (Stephens et al., 2002) were used for these positions.

Gravity cores In the laboratory in Bremen, the samples were washed over a 150μm and a 63μm sieve and dried at 50°C. As for the multicorer samples, a binocular microscope was used to find individuals of *O. umbonatus*. But unlike in the multicorer

samples, it was not possible, to find at least five individuals in each gravity core sample, so that it was necessary to measure smaller amounts of tests and/or combine two adjoining core-depths in these cases.

1.4.3. Trace element determination by laser ablation ICP-MS

A Finnigan Laserprobe UV (266nm wavelength) laser ablation system, coupled to a Finnigan Element 2 sector field ICP-MS was used for the trace element analyses. The calibrations are based on the NIST610 glass standard reference material (SRM), assuming the composition according to Pearce et al. (1997).

The foraminifers were fixed on a sample holder with double-sided duct tape and placed in the ablation chamber. The ablated material was transported out of the chamber with a helium flow of 0.36l/min. For the final sample gas, argon was admixed. For ablation we used a laser beam with 1.2mJ energy and a pulse rate of 5Hz. Beam diameters were 50μm for the standards and $\sim 70\mu$m for the foraminifers. The different diameters were necessary to account for differences in the ablation behavior. Data acquisition time was 80s (including blank signal), about $20 - 30$s of the signal were used for trace element quantification. Elemental concentrations were determined on the isotopes ^{25}Mg, ^{43}Ca and ^{88}Sr, where Ca was used as internal standard (assuming a Ca concentration of $40.04\%wt$). Errors in the assumed Ca content can lead to errors in the estimate of the absolute Mg and Sr content in the shell, but not in the calculated ratios. ^{55}Mn and ^{64}Zn were measured as indicators of contaminants. The high energy density and the long acquisition time resulted in regular penetrations of the foraminiferal tests on one side. However, measurements of Zn, which is present in the adhesive tape that was used as sample holder, indicate that the duration of the ablation process was not sufficient to entirely penetrate the foraminiferal shell. Mn is present in both, clay minerals and iron-manganese crusts. No corrections have been applied for raised concentrations of Mn, but major contributions of contaminants to the analyses were avoided by carefully selecting the time-resolved sample signal in each measurement run. Each foraminiferal test was measured five times on different positions. The NIST610 standard was measured before and after each foraminiferal test. For each sample location, the final Mg/Ca ratio was calculated by averaging the up to 50 measurements (5 points per specimen, up to 10 specimens per sample). This procedure makes up for the high within- and between-shell variability for Mg/Ca (Rathmann et al., 2004). The standard errors of the averages range from 0.1 to 0.4mmol/mol for Mg/Ca, and from 0.01 to 0.03mmol/mol for Sr/Ca. Figure 1.7 shows an example for a foraminifera after the measurement.

For calibration, only the 2σ range of all measurements from each core top sample was used.

1.4.4. Stable isotope determination by ICP-MS

Stable isotopes were measured after the trace element measurements on the same shells. The foraminiferal tests were removed from the adhesive tape with a wet brush and than prepared for the stable isotope measurements. Stable carbon isotopes ($\delta^{13}C$) and stable oxygen isotopes ($\delta^{18}O$) were determined on a Finnigan MAT 251 mass spectrometer equipped with an automated carbonate device. The analytical errors

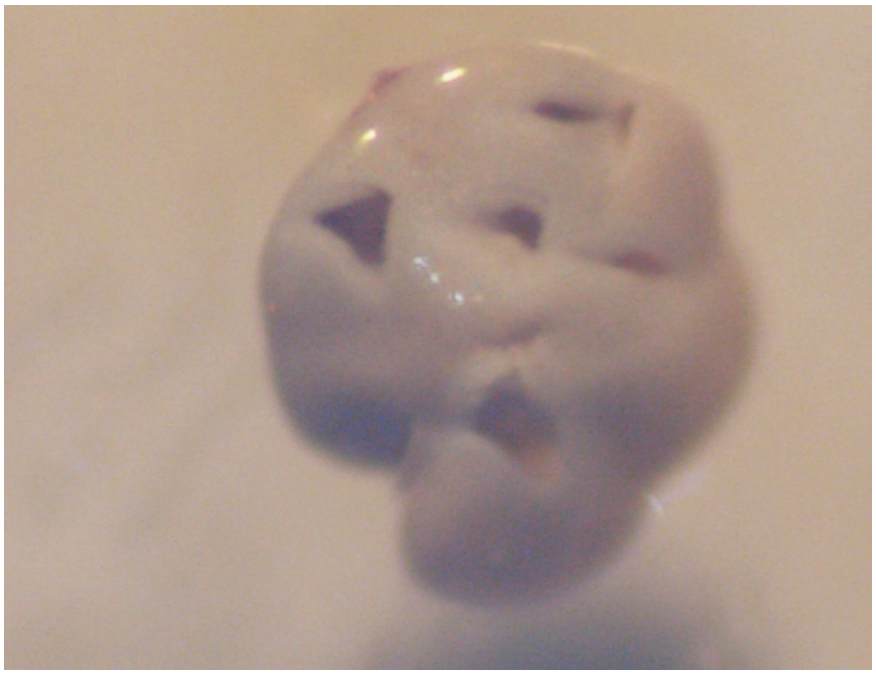

Figure 1.7.: Lasered foraminifera.

(1σ) are 0.07 for $\delta^{18}O$ and 0.03 for $\delta^{13}C$. The reproducibilities based on a laboratory standard are < 0.09 for $\delta^{18}O$ and < 0.05 for $\delta^{13}C$. To investigate the potential impact of laser ablation on the stable isotopic composition (for example, due to fractionation in the vapour and subsequent condensation on the sample), we additionally measured fresh (not ablated) sample splits for M57/2. Each of these parallel splits consisted of five tests.

1.4.5. Geochemical properties

Geochemical analyses of the pore-water were carried out onboard the research vessel by the geochemistry group of the Geosciences Department of Bremen University directly after recovery to prevent sample alteration. Pore-water samples were squeezed from the same or parallel multicorer as the foraminifer samples. Titration with 0.01, 0.05 or $0.1M$ HCl was used to determine alkalinity, and pH was measured with an electrode before the sediment structure was disturbed. The analytical errors are better than 3% for alkalinity and 0.05 for pH. Data were provided by C. Hensen (GeoB 17xx and 37xx, available at the WDC-Mare database) and M. Zabel (GeoB 84xx, personal communication, 2006). Measurements were performed at the sediment surface and at 3 or 7mm sediment depth.

1.4.6. XRF-scanning

In the laboratory in Bremen the archive half of the gravity cores was used to measure the elemental concentrations with an XRF-scanner. The Fe-counts of these measurements were used for the correlation of the gravity cores. A significant peak in the Fe-counts was used to identify the LGM.

The XRF core scanner allows a nondestructive, nearly continuous, and relatively fast analysis of various elements. The XRF scanner measures the chemical composition of the sediment as element intensities in total counts (cnts) or counts per second (cps), which are proportional to the chemical concentrations. Although element intensities mainly depend on the element concentration, they are also influenced by the energy level of the X-ray source, the count time, and the physical properties of the sediment. Conventional XRF analyzers use dry and homogenized powder samples in order to avoid interference of sample inhomogeneities or physical variations. However, down-core varying physical properties can be an issue for XRF core scanner analyzes that are obtained directly at the split core surface. A more detailed study about different influences on the XRF-measurement quality was conducted by Tjallingii et al. (2007).

1.5. Outline

The presented thesis will contribute to a better knowledge of benthic foraminifera and the use of their trace element ratios and stable isotopes for paleoceanographic reconstructions. The development of new proxies and the improvement of existing ones are essential for a better understanding of the climate history.

In the first manuscript, "Mg/Ca ratios of the benthic foraminifera *Oridorsalis umbonatus* obtained by laser ablation from core top sediments: Relationship to bottom water temperature" (Söhnke Rathmann, Silvia Hess, Henning Kuhnert and Stefan Mulitza, published in Geochemistry Geophysics Geosystems), a regional calibration for the Mg/Ca–BWT-relationship on *O. umbonatus* obtained by laser ablation ICP-MS is presented. The samples from the topmost cm from six multicores on a transect from a water depth of 320m down to 2293m off Lüderitz were investigated. Five to seven tests of the benthic foraminifera *O. umbonatus* were measured for their trace element ratios using a laser ablation ICP-MS system. The resulting exponential equation for the Mg/Ca–BWT-relationship ($\mathrm{Mg/Ca} = 1.528 * e^{0.09*\mathrm{BWT}}$) is similar to comparable ones for other species, which confirms the usefulness of *O. umbonatus* in the reconstruction of BWTs. This regional calibration is the basis for ongoing research in this area (see the following manuscripts).

In the second manuscript, "Carbonate ion effect on Mg/Ca, Sr/Ca and stable isotopes on the benthic foraminifera *Oridorsalis umbonatus* off Namibia" (Söhnke Rathmann and Henning Kuhnert, published in Marine Micropaleontology), the modern reference dataset is improved with 4 additional multicores (one to close the gap between 605m and 1330m water depth and 3 to extend the depth range down to 4004m water depth). The dependence of Mg/Ca, Sr/Ca, $\delta^{18}O$ and $\delta^{13}C$ on the BWT, pH, $[CO_3^{2-}]$ and $\Delta[CO_3^{2-}]$ (both from the pore-water and the water column for the last 3 parameters) was investigated on the samples. A correlation between Sr/Ca ratios and $[CO_3^{2-}]$ as well as between shell $\delta^{18}O$ (corrected for temperature and $\delta^{18}O_{seawater}$) and $[CO_3^{2-}]$ was observed, however, the variability of the corrected $\delta^{18}O$ is close to the analytical limit. Mg/Ca and $\delta^{13}C$ showed no clear dependences on $[CO_3^{2-}]$. Neither the trace element ratios nor the stable isotopes had a dependence on $\Delta[CO_3^{2-}]$. Interestingly, these results support the results from Elderfield et al. (2006), who also found no relationships with $\Delta[CO_3^{2-}]$ and only relationships with $[CO_3^{2-}]$ in the South

Atlantic.

For the third manuscript, "Stratification of eastern South Atlantic (25°S) upper water masses during the Last Glacial Maximum" (Söhnke Rathmann, Henning Kuhnert, André Paul, Oscar Romero and Stefan Mulitza, manuscript in preparation for submission), gravity cores from the positions of the aforementioned multicores were examined. The cores were correlated with each other using the Fe-content, investigated using the XRF-scanning method, and a horizon (LGM) was chosen for the paleoceanographic application of Mg/Ca ratios of *O. umbonatus*. These horizons were measured, and a comparison of LGM and modern temperatures was made. Interestingly, we found no lower BWTs as expected for the LGM. On the contrary, we even found slightly higher temperatures. This is contrary to the changes in the SSTs, as described by Niebler et al. (2003), who used a modified version of the Imbrie-Kipp-Transfer-Function for their analyses and found that the LGM SSTs were up to 10°C lower than today.

2. Mg/Ca ratios of the benthic foraminifera *Oridorsalis umbonatus* obtained by laser ablation from core top sediments: Relationship to bottom water temperature

Söhnke Rathmann, Silvia Hess, Henning Kuhnert and Stefan Mulitza
Geochem. Geophys. Geosys. **5** (2004) Q12013, doi:10.1029/2004GC000808

Abstract A laser-ablation system connected to an inductively coupled plasma mass spectrometer was used to determine Mg/Ca ratios of the benthic foraminifera *Oridorsalis umbonatus*. A set of modern core top samples collected along a depth transect on the continental slope off Namibia ($320 - 2300$m water depth; $2.9°$ to $10.4°$C) was used to calibrate the Mg/Ca ratio against bottom water temperature. The resulting Mg/Ca–bottom water temperature relationship of *O. umbonatus* is described by the exponential equation: $\mathrm{Mg/Ca} = 1.528 * e^{0.09 * \mathrm{BWT}}$. The temperature sensitivity of this equation is similar to previously published calibrations based on *Cibicidoides* species suggesting that the Mg/Ca ratio of *O. umbonatus* is a valuable proxy for thermocline and deep water temperature.

Keywords: benthic foraminifera, Mg/Ca thermometry, laser ablation ICP-MS, trace elements, temperature, marine geochemistry

2.1. Introduction

Mg/Ca ratios of benthic foraminiferal tests have been used as a proxy for bottom water temperatures (Rathburn and De Deckker, 1997; Rosenthal et al., 1997; Lea, 1999; Lear et al., 2000, 2002; Martin et al., 2002; Billups and Schrag, 2003). The most commonly used species is *Cibicidoides wuellerstorfi* which is adapted to oligotrophic deep sea conditions (Corliss, 1985; Lutze and Thiel, 1989; Corliss, 1991; Gooday, 1994). *Cibicidoides wuellerstorfi* is an epifaunal taxon and has been observed to live in microhabitats at the sediment/water interface. However, in shallow water depths (above ~ 1000m) and in highly productive areas, *C. wuellerstorfi* can be extremely rare or even absent (Lutze and Thiel, 1989; Schmiedl, 1995). Hence calibrations for other species are needed, especially if thermocline properties are to be

reconstructed. The species *Oridorsalis umbonatus* represents a potential alternative to *C. wuellerstorfi*. *Oridorsalis umbonatus* is a preferentially shallow infaunal living species (Corliss, 1985; Rathburn and Corliss, 1994; Schmiedl et al., 1997), occurring in a wide range of habitats and water depths. Its long geological record spanning the entire Cenozoic (Lear et al., 2000) makes this species particularly useful as a recorder of paleoenvironmental conditions.

Generally, the two main strategies to determine trace elemental composition in foraminifera are based on the analysis of liquid solution of dissolved shells and laser ablation of solid shells. For liquid solution analysis, the foraminifer samples undergo an elaborate cleaning procedure (Martin and Lea, 2002; Barker et al., 2003) and are subsequently dissolved in diluted acid. The solution is usually analyzed by inductively coupled plasma atomic emission spectrometer (ICP-AES) or inductively coupled plasma mass spectrometer (ICP-MS) (Rosenthal et al., 2004). The advantages of this method are the perfect sample homogenization and high analytical precision. Laser ablation requires no or minimal sample preparation. Material is directly ablated from the foraminiferal test and is introduced to an ICP-MS (Eggins et al., 2003; Hathorne et al., 2003; Reichart et al., 2003). The laser beam can also be used to remove surface contamination from the shell prior to analysis. The advantages of this method are the absence of time-consuming preparation and the small sample size needed for analyses (theoretically less than a single shell). The absence of a chemical treatment also precludes the alteration of the analyzed material. However, comparisonof Mg/Ca ratios in coral samples measured by laser ablation and by isotope dilution ICP-MS showed no systematic offsets (Fallon et al., 1999).

Here, we used the laser ablation technique to measure Mg/Ca ratios of *O. umbonatus* from the continental slope off Namibia. Our data show that the slope of the Mg/Ca–temperature relationship of *O. umbonatus* is very close to that of *C. wuellerstorfi*. Hence Mg/Ca in *O. umbonatus* is a useful proxy to estimate past variations in bottom water temperatures.

Table 2.1.: Sample Position, Water Depth, Bottom Water Temperature, and Mg/Ca Ratio of Individual Tests of *Oridosalis umbonatus*[a]

Sam-	Lat.,	Lon.,	WD,	BWT,	Mean Mg/Ca Ratio, mmol/mol																				
					1			2			3			4			5			6			7		
ple	°S	°E	m	°C	∅	Max, Min	N^o	∅	Max, Min	N^o	∅	Max, Min	N^o	∅	Max, Min	N^o	∅	Max, Min	N^o	∅	Max, Min	N^o	∅	Max, Min	N^o
GeoB 8403-1	24.25	13.61	320	10.41	4.13	4.87, 3.36	4	3.94	4.61, 2.93	4	3.70	4.58, 2.67	5	4.74	5.95, 3.64	5	3.34	3.73, 2.91	5						
GeoB 8452-1	25.46	13.68	388	8.43	3.09	4.05, 2.73	5	3.11	3.46, 2.92	5	3.43	4.25, 2.72	5	4.16	5.02, 3.78	4	2.95	3.42, 2.31	5						
GeoB 8450-1	25.47	13.61	506	6.42	2.06	2.39, 1.91	5	2.71	3.37, 2.37	4	3.09	3.37, 2.78	5	2.01	2.3, 1.62	4	2.54	2.98, 2.1	5	2.09	2.29, 1.94	4	2.83	4.05, 2.33	5
GeoB 8449-1	25.48	13.55	605	5.52	2.81	3.33, 2.49	4	1.98	2.15, 1.86	5	2.92	4.16, 2.24	5	3.07	3.78, 2.6	5	2.33	2.91, 1.8	5	3.07	3.42, 2.73	5			
GeoB 8430-2	25.61	13.28	1330	3.33	2.11	2.36, 1.87	3	1.85	2.4, 1.58	5	2.06	2.48, 1.79	5	1.69	2.38, 1.36	5									
GeoB 8462-4	25.54	12.95	2293	2.91	2.25	3.31, 1.86	5	1.69	2.17, 1.35	5	3.53	4.27, 2.7	4	1.10	1.41, 0.9	5	1.28	1.36, 1.2	5	3.53	4.45, 1.95	4			

[a] WD, water depth; BWT, bottom water temperature. Outliers ($> 2\sigma$) were excluded for Mg/Ca.

2.2. Material and Methods

2.2.1. Sampling

We used multicorer samples from the Benguela upwelling system off Namibia from a water depth range of 320 to 2300m collected during METEOR cruise M57/2 (Zabel and cruise participants, 2003). Immediately after recovery, the sediment cores were cut into $1cm$ slices, preserved and stained with an ethanol/Rose Bengal solution. The multicorer samples were washed over a 125μm and a 63μm sieve and dried at $50°$C. For Mg/Ca measurements five to seven individuals of *O. umbonatus* with a diameter of $300 - 400\mu$m were collected from the topmost centimeter of the sediment of six stations (Table 2.1). Only well-preserved tests (with all chambers) were used. In all samples, Rose Bengal stained shells were present, which indicates modern sediments. Furthermore the $\delta^{18}O$ composition of the planktic foraminifer *Neogloboquadrina pachyderma* (dex.) from the same sample is close to Holocene values from nearby cores (S. Rathmann, unpublished data, 2003) supporting the modern age of the samples.

For each multicorer position, temperature profiles were measured with a conductivity-temperature-depth probe (CTD SBE 911+) (Moorholz and Heene, 2003a). The measured bottom water temperature (BWT) at the investigated sites covers a range of $2.9°$ to $10.4°$C (Tables 2.1 and 2.2). Generally, the CTD temperatures measured in the field are well within the seasonal temperature range derived from the World Ocean Atlas (WOA) (Levitus and Boyer, 1994; Stephens et al., 2002) for the site loca-

Table 2.2.: Comparison of Bottom Water Temperature Between CTD Measurements and Data From the World Ocean Atlas 1994 and 2001 for the Core Locations[a]

Water depth, m	Mean Mg/Ca Ratios	CTD Temp. °C	WOA (1994) Temp. °C			WOA (2001) Temp. °C		
			Mean	Max.	Min.	Mean	Max.	Min.
320	3.96	10.41	9.28	9.84	8.85	9.14	9.43	8.74
388	3.31	8.43	8.13	8.64	7.77	8.03	8.35	7.59
506	2.50	6.42	6.10	6.53	5.71	6.22	6.55	5.85
605	2.69	5.52	5.09	5.57	4.74	5.37	5.66	4.82
1330	1.91	3.33	3.28	3.32	3.26	3.31	3.42	3.22
2293	2.14	2.91	3.02	3.03	3.00	2.99	3.03	2.97

[a] Levitus and Boyer (1994); Stephens et al. (2002) ($<$ 1000m wd: monthly, $>$ 1000m wd: seasonal).

tions, except for the shallowest site, where measured temperatures were more than $1°$C higher than the warmest temperature estimated in WOA. We attribute this mismatch to the interpolation technique used in WOA, which fails to reproduce very strong temperature gradients associated to hydrographic fronts and small-scale hydrographic features (Schäfer-Neth et al., 2005).

2.2.2. Analytical methods

Mg/Ca measurements were done with a Finnigan Laserprobe UV (266nm wavelength) laser ablation system, coupled to a Finnigan Element 2 sector field ICP-MS. The cali-

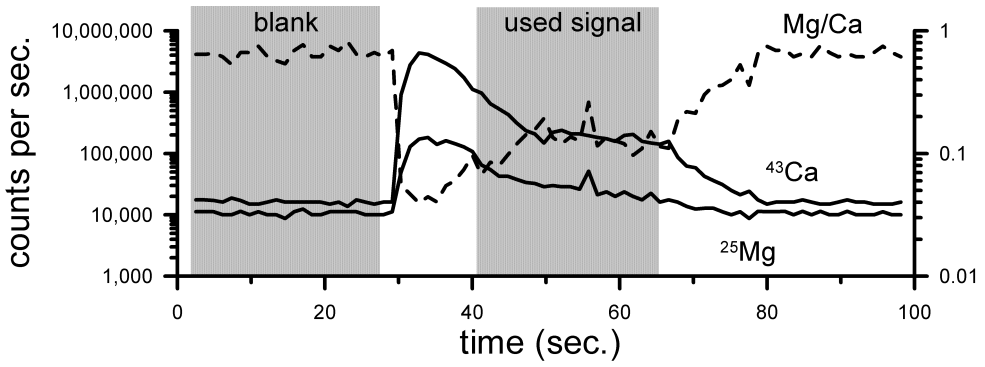

Figure 2.1.: Signal intensity of Mg and Ca versus time for a typical measurement.

brations are based on the NIST610 glass standard reference material (SRM) (provided by the USGS), assuming the composition according to Pearce et al. (1997).

The foraminifers were fixed on a sample holder with double-sided duct tape and placed in the ablation chamber. The ablated material was transported out of the chamber with a helium flow of 0.36l/min. For the final sample gas, argon was admixed. For ablation we used a laser beam with 1.2mJ energy and a pulse rate of 5Hz. Beam diameters were 50μm for the standards and $\sim 70\mu$m for the foraminifers. The different diameters were necessary to account for differences in the ablation behavior. Data acquisition time was 80s (including blank signal), about $20 - 30$s of the signal were used for trace element quantification (Figure 2.1). Elemental concentrations were determined on the isotopes ^{25}Mg and ^{43}Ca, where Ca was used as internal standard (assuming a Ca concentration of $40.04\%wt$). Errors in the assumed Ca content can lead to errors in the estimate of the absolute Mg content in the shell, but not in the Mg/Ca ratios. For this reason, we report the latter. The high energy density and the long acquisition time resulted in regular penetrations of the foraminiferal test on one side. However, we did not observe a complete penetration of a specimen otherwise the laser beam would ablate the adhesive tape or the sample holder. Measurements of ^{66}Zn, which is present in the tape and in the sample holder, indicate that the duration of the sampling was not sufficient to entirely penetrate the foraminiferal shell. Each foraminiferal test was measured five times at different locations. The NIST610 standard was measured before and after each foraminiferal test. For each sample location, the final Mg/Ca ratio was calculated by averaging $25 - 35$ measurements (5 points per specimen, $5 - 7$ specimens per sample).

In order to assess the reproducibility of our data we measured the NIST610 standard and a pellet prepared from the coral powder standard JCp-1 (Okai et al., 2002). The aragonitic JCp-1 has a chemical composition comparable to that of calcitic foraminiferal tests. The NIST610 and JCp-1 were treated as "samples", each five samples a measurement of the NIST610 treated as "standard" was inserted for calibration.

The measurements of the NIST610 glass show a relative standard deviation of 0.65% (based on 10 replicates). For the carbonate powder JCp-1 we obtained a relative standard deviation of 3.8% (based on 20 replicates). This suggests that the precision of the measurements is limited by sample inhomogeneities rather than by instrumental precision.

The Mg/Ca ratio for JCp-1 derived from our measurements is 3.79mmol/mol, which

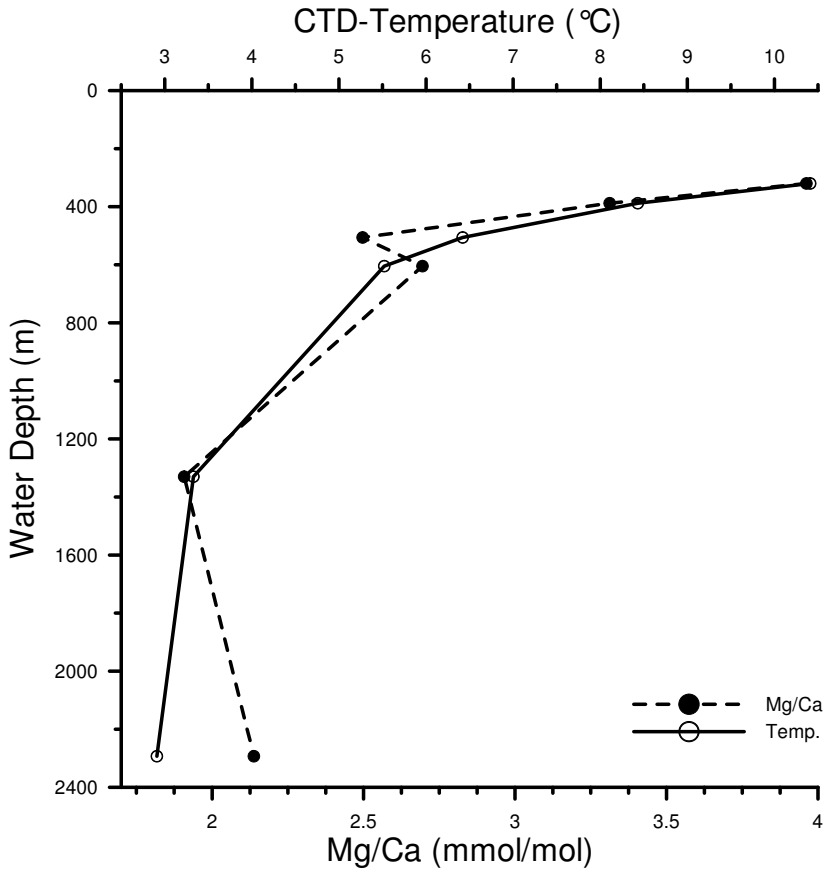

Figure 2.2.: Mg/Ca and CTD bottom water temperature at the sampling sites versus depth. Values are reported in Table 2.2.

is 10% less than the value of 4.20mmol/mol reported by Okai et al. (2002). This difference is probably introduced by using a silicate standard for calibration, which is not matrix-matched compared to the carbonaceous JCp-1; this may lead to differences in the behaviour of both materials in the plasma. For calibration, we only used the 2σ range of all measurements from each core top sample. All data are available from the WDC-Mare database (http://www.wdc-mare.org/PangaVista? query=@Ref26032).

2.3. Results

The core top samples measured here correspond to a temperature range of about 7°C from about 10°C at 320m depth to about 3°C at 2300m depth. Generally, Mg/Ca ratios averaged for all measurements of *O. umbonatus* from the same sample decrease with lower bottom-water temperatures and greater water depths (Figure 2.2 and Table 2.2). Lowest Mg/Ca ratios ($\sim$ 2mmol/mol) of core top means are encountered in the samples GeoB 8462-2 (2293m water depth) and GeoB 8430-2 (1330m water depth), the highest Mg/Ca ratios ($\sim$ 4mmol/mol) correspond to the shallowest sample at the warm end (GeoB 8403-1, 320m water depth).

There is considerable scatter in the Mg/Ca ratios between individuals of *O. umbonatus* from the same sample and also between measurements from different positions

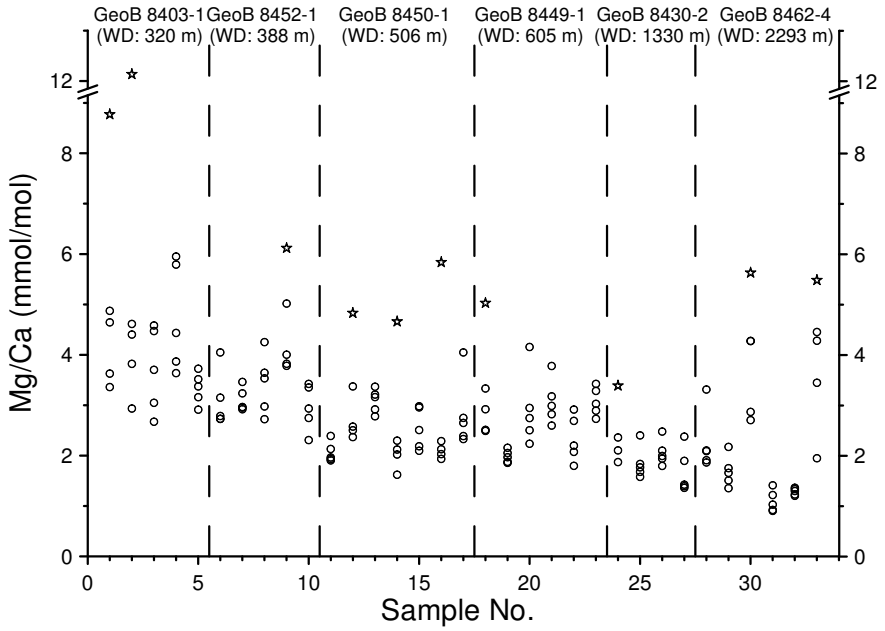

Figure 2.3.: Mg/Ca ratios (mmol/mol) of individual measurements on single shells of *O. umbonatus*. Asterisks denote data outside the 2σ range not used for calibration in Figures 2.5 and 2.6.

within the same shell. The highest variability within and between individual shells occurs in the shallowest sample GeoB 8403-1. The salient features in this sample are two extreme outliers with Mg/Ca ratios of 8.77mmol/mol and 12.13mmol/mol (Figures 2.3 and 2.4). The standard deviation of the Mg/Ca ratios within single shells of *O. umbonatus* varied between 0.07 and 3.72. The average standard deviation between mean values of shells from the same core top sample varied between 0.35 and 1.12.

The polynomial regression of the mean Mg/Ca ratios versus bottom water temperature (BWT) yields the equation: $\mathrm{Mg/Ca} = 1.528 * e^{0.09*\mathrm{BWT}}$ (Figure 2.5). The slope of this Mg/Ca–temperature relationship is similar to that found for *Cibicidoides* spp. (Rosenthal et al., 1997; Martin et al., 2002) and *O. umbonatus* (Lear et al., 2002) in the same temperature range. However, the absolute Mg/Ca ratios predicted by our equation are significantly higher than indicated by the relationships of Lear et al. (2002) and Martin et al. (2002) (Figures 2.5 and 2.6). For example, our equation would estimate about $1.5° - 3.6°$C cooler temperatures than the *O. umbonatus* equation from Lear et al. (2002) and about $0.3° - 2.1°$C cooler temperatures than the *Cibicidoides* spp. equation published by Martin et al. (2002).

2.4. Discussion

2.4.1. Variability within shells

Our data indicate that the Mg/Ca composition of *O. umbonatus* is not homogenous. In all core top samples, up to 3 outliers with a significantly higher Mg/Ca ratio than the majority of the measurements occur. Toyofuku et al. (2000) argue that chambers of benthic foraminifera which were build incrementally can have different Mg/Ca ratios

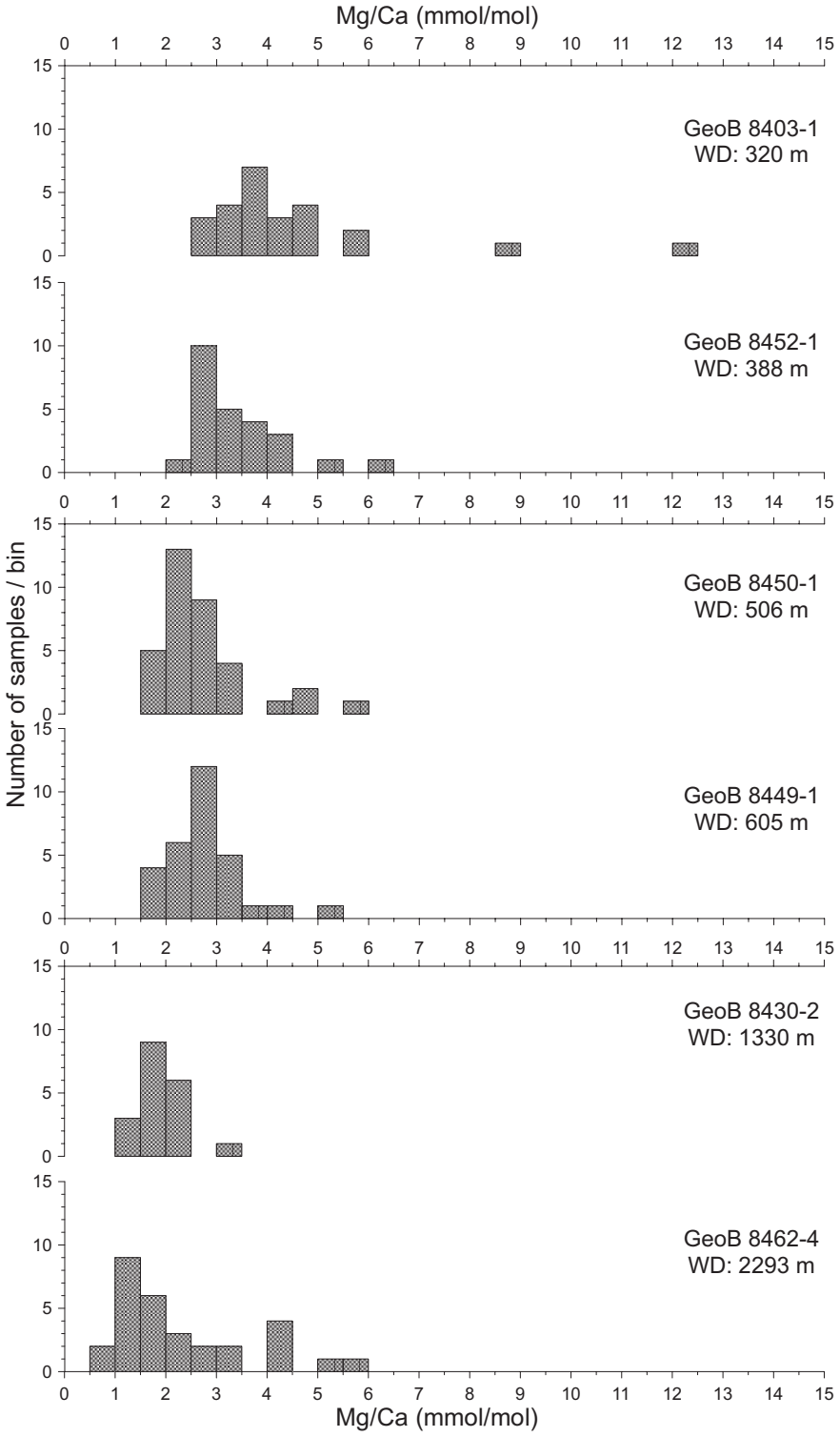

Figure 2.4.: Histograms of the measured Mg/Ca ratios. Classes correspond to a temperature difference of $\sim 1°C$

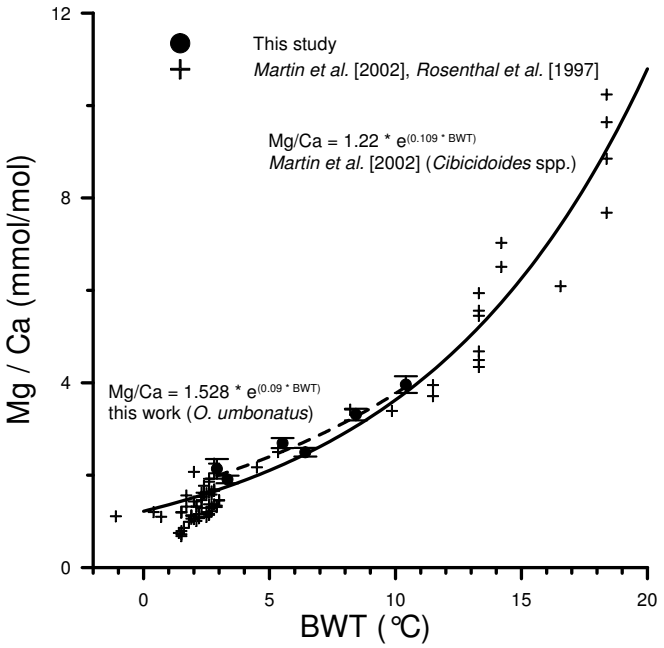

Figure 2.5.: Comparison of mean Mg/Ca ratios of *O. umbonatus* of our data (dots) with data from Martin et al. (2002) (BWT $< 4°$C) and Rosenthal et al. (1997) (BWT $> 4°$C) (crosses). Vertical bars indicate standard errors of all measurements from one core top sample. Outliers (see Figure 2.4) were not included. BWT for our samples has been derived from local CTD measurements at the sampling positions.

at different times of the year due to seasonal temperature variations. For the extreme outliers observed in core top GeoB 8403-1, the maximum difference between Mg/Ca ratios measured on the same shell would correspond to a temperature difference of about $20°$C using the slope of Martin et al. (2002). Since the seasonal temperature variations are on the order of $< 0.1°$C in deep water masses and up to $1.0°$C in shallow water masses, local variations in temperature do not explain the observed magnitude of the variability within and between shells.

Another explanation might be vital effects due to variations of the carbonate chemistry in the microenvironmentof the shell. For example Eggins et al. (2004) have shown that the Mg/Ca ratios within the test of the planktonic foraminifer *Orbulina universa* is composed of several growth bands with variations in the Mg/Ca ratio up to 200%. They suggest that variations in pH in the vicinity of the shell due to changes in photosynthesis, respiration and calcification rate (Lea et al., 1999; Eggins et al., 2004) are the reason forthe observed variability in Mg/Ca ratios. Wolf-Gladrow et al. (1999) have shown that calcification alone can lower the pH in the vicinity of foraminiferal shells with respect to that of ambient seawater. Hence an increase of calcification rate only, e.g., due to increase food supply, might decrease the pH in the microenvironment of *O. umbonatus* which would lead to increased Mg/Ca ratios at least in parts of the shell. However, future studies must show whether a layering of Mg/Ca ratios is also present in non-symbiotic benthic foraminifera.

Finally, the more extreme deviations can be due to contaminations with high Mg-calcite growing in the interior of the shell and/or sediment fillings. While contamina-

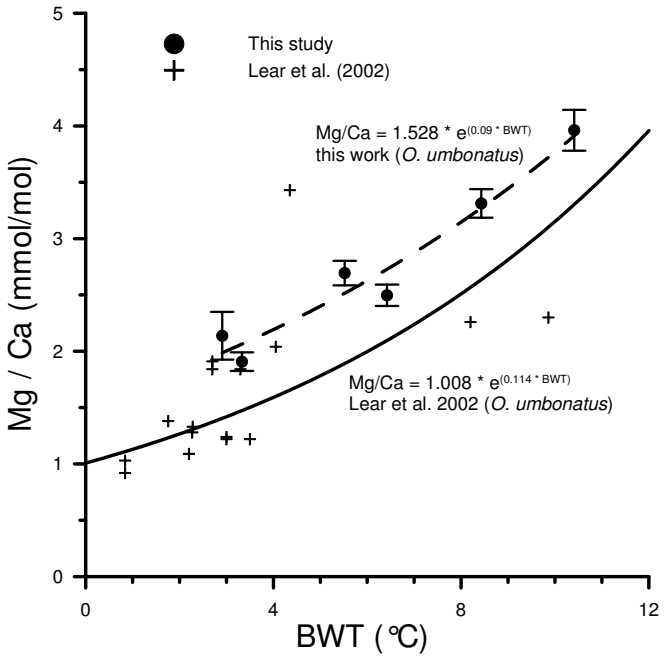

Figure 2.6.: Comparison of mean Mg/Ca ratios of *O. umbonatus* of our data (dots) with data from Lear et al. (2002) (crosses). Vertical bars indicate standard errors of all measurements from one core top sample. Outliers (see Figure 2.4) were not included. BWT for our samples has been derived from local CTD measurements at the sampling positions.

tions on the exterior of the shell were avoided during sampling, we had little control on potential contaminations within the chambers. Since the laser beam regularly penetrated the outer shell, chamber fillings would bias the measured signal.

One strategy to exclude the outliers is to use only the 2σ range of the data which should comprise about 95% of the entire data set. This approach would reduce the standard error (based on standard deviations of 0.34 to 1.11) of the mean Mg/Ca of our samples to values between 0.08 (GeoB 8430-2) and 0.21 (GeoB 8462-4), which would correspond to a reproducibility of the mean of about $\pm 0.3°$ to $\pm 0.8°$C.

2.4.2. Comparison to other Mg/Ca-Temperature Relationships

The absolute Mg/Ca ratios of our data are about $0.2 - 0.3$mmol/mol higher than indicated by the Mg/Ca–temperature relationship for *Cibicidoides* spp. published by Martin et al. (2002). Interestingly, the mean difference is close to the mean difference calculated for downcore measurements of *O. umbonatus* and *Cibicidoides wuellerstorfi* (Lear et al., 2000). Hence these higher Mg/Ca ratios in our data might simply be explained by species specific vital effects.

Another reason might be the cleaning procedure applied to liquid solution Mg/Ca measurements. For example, Barker et al. (2003) found that the Mg/Ca ratios were reduced through the cleaning procedure by up to $10 - 15\%$. Since our samples have not been cleaned our results should indeed be higher. However, unpublished intercalibra-

tions of sample material measured with both by laser ablation and from liquid solution show no systematic offset for the benthoc species *Cibicides pachyderma* (S. Weldeab, unpublished data, 2004). This would impl a minor effect of the cleaning procedure on the Mg/Ca ratio of benthic foraminifera. However, future intercalibrations on other benthic species must show whether this finding can be generalized.

The best documented benthic relationship for Mg/Ca vs. temperature has been derived for *Cibicidoides* species in the temperature range between $-1°$ and $19°$C (Martin et al., 2002). Although our data set has been produced by a different methodology, the slope of the relationship of Martin et al. (2002) is nearly identical to that derived in this work. For example, Mg/Ca temperature in our relationship is about 0.22 per °C between $0°$ and $10°$C, whereas Martin et al. (2002) indicates a slope of about 0.24 per °C in the same temperature range.

Mg/Ca data for *O. umbonatus* are available from a set of core tops from different ocean basins (Lear et al., 2000). These measurements indicate that the Mg/Ca relationship of *O. umbonatus* is less well constrained than for other benthic species. For example, individual measurements of Mg/Ca deviate up to 1.78mmol/mol ($\sim 6°$C) from a polynomial fit through the data. Our calibration does not show such a large variability. This may indicate that regional calibrations give more consistent results than calibrations based on material from different oceans.

2.5. Conclusions and paleoceanographic implications

Measuring Mg/Ca ratios with the laser ablation technique on *O. umbonatus* is an alternative approach to estimate bottom water temperature. Our results show that the sensitivity of the Mg/Ca–temperature relationship for *O. umbonatus* is comparable to that of *Cibicidoides* spp. Since *O. umbonatus* is abundant over the main thermocline, it provides a good candidate for studying past variations in vertical temperature gradients.

The laser ablation technique allows the rapid determination of Mg/Ca ratios as long as the number of samples is relatively small. It is therefore well suited for overviews on core sequences and can serve as a base for subsequent high-resolution studies with liquid solution analyses. Laser ablation also provides information on within-sample variability that is otherwise difficult to obtain. Furthermore, the high number of measurements per sediment sample allows identification of outliers and potentially contaminated shell parts, increasing the accuracy of the final temperature estimate.

Acknowledgements We thank Andreas Klügel for improving the instrument setup. Thanks to S. Weldeab, P. De Deckker, A. Jurkiw and G. Wefer for discussion and two anonymous referees for constructive comments. This work was funded by the Deutsche Forschungsgemeinschaft (DFG Research Center Ocean Margins contribution RCOM0209) and the Bundesministerium für Bildung und Forschung (DEKLIM).

3. Carbonate ion effect on Mg/Ca, Sr/Ca and stable isotopes on the benthic foraminifera *Oridorsalis umbonatus* off Namibia

Söhnke Rathmann and Henning Kuhnert
Marine Micropaleontology **66** (2008) 120–133

Abstract We investigate the influence of carbonate system parameters (carbonate ion concentration, [CO_3^{2-}], carbonate ion saturation, $\Delta[CO_3^{2-}]$) on the trace element and stable isotope ratios in the endobenthic foraminifera *Oridorsalis umbonatus*. Data from modern core top samples from the Namibian continental slope suggest that the shell composition of this species is influenced by the chemistry of the pore-water. For these organic-rich sediments, the impact of ocean bottom water properties on both pore-water and shell chemistry is surprisingly small. Sr/Ca correlates negatively with [CO_3^{2-}] and to a lesser extend to $\Delta[CO_3^{2-}]$, which is opposed to previous results. A [CO_3^{2-}] decrease of 10μmol/kg leads to an increases of 0.05mmol/mol in Sr/Ca. We observe a correlation between shell $\delta^{18}O$ (corrected for temperature and $\delta^{18}O$seawater) and [CO_3^{2-}], however, the variability of the corrected $\delta^{18}O$ is close to the analytical limit. No clear dependences were observed for $\delta^{13}C$ and Mg/Ca.

Keywords: benthic foraminifera, stable isotopes, laser ablation ICP-MS, trace elements, temperature, carbonate ion effect

3.1. Introduction

The elemental ratios of Mg/Ca and Sr/Ca, and the stable isotopic composition ($\delta^{18}O$, $\delta^{13}C$) of foraminifera tests are among the most often used proxies in paleoceanography. With the exception of Sr/Ca, the primary environmental controls on these parameters are well known. Mg/Ca is driven by temperature (Rathburn and De Deckker, 1997; Rosenthal et al., 1997; Lea, 1999; Lear et al., 2000, 2002; Martin et al., 2002; Billups and Schrag, 2003), $\delta^{18}O$ by temperature and $\delta^{18}O$ of seawater (e.g., Emiliani, 1955; Shackleton, 1974), and $\delta^{13}C$ by a multitude of factors including $\delta^{13}C$ of seawater, bottom water circulation and vital effects (e.g., Broecker and Peng, 1982; Mackensen and Bickert, 1999). Sr/Ca is marginally influenced by temperature (Müller, 2000; Mortyn et al., 2005), but seems to be driven by the carbonate ion concentration

and the carbonate saturation state ($\Delta[CO_3^{2-}]$, the difference between [CO_3^{2-}] and saturation [CO_3^{2-}]) of the ambient water for some species (Lea et al., 1999; Russell et al., 2004; Mortyn et al., 2005; Rosenthal et al., 2006) and, on the glacial to interglacial timescale, by changes in the Sr/Ca of seawater (Stoll et al., 1999). The other three proxies are also influenced to varying degrees by changes in [CO_3^{2-}] and $\Delta[CO_3^{2-}]$, often referred to as the carbonate ion effect.

For stable isotopes this has been shown for planktonic foraminiferal species in culturing experiments (Spero et al., 1997; Wolf-Gladrow et al., 1999; Zeebe, 1999; Zeebe et al., 1999) and in samples from sediment traps and multinets (Russell and Spero, 2000; Wilke et al., 2006). Studies on the elemental composition have been carried out on cultured planktonic (Lea et al., 1999; Russell et al., 2004), and benthic species from sediment core tops (Rosenthal et al., 2006; Elderfield et al., 2006).

For planktonic and epibenthic foraminifera ambient [CO_3^{2-}] is governed by the properties of the water column. However, for endobenthic foraminifera [CO_3^{2-}] is determined by the pore-water, the composition of which may significantly deviate from that of the bottom water. Elderfield et al. (2006) showed that the effect of bottom water $\Delta[CO_3^{2-}]$ on shell Mg/Ca was significantly larger in the epibenthic *Cibicidoides wuellerstorfi* than in endobenthic *Uvigerina* spp. They argued that the pore-water approaches the $CaCO_3$ equilibrium ($\Delta[CO_3^{2-}]$=0) with increasing sediment depth (on the order of magnitude of a few centimetres) and that foraminifera calcifying below the equilibrium depth would not be subject to $\Delta[CO_3^{2-}]$ effects.

However, close to the sediment-bottom water interface, the carbonate chemistry of the pore-water can be influenced by the oxidation of organic matter, and the release of metabolic CO_2 leads to more acidic pH and lower [CO_3^{2-}] (Archer et al., 1989; Hales and Emerson, 1996). Foraminifera growing in this uppermost sediment layer should therefore exhibit a characteristic pore-water signature in their shell chemistry. The carbonate ion effect, if present, should be identifiable in Mg/Ca, Sr/Ca, and $\delta^{18}O$; for $\delta^{13}C$ the situation is more complex, as it is also influenced by the isotopic composition of the pore-water.

An ideal location to investigate the relationship between benthic foraminiferal shell composition and pore-water [CO_3^{2-}] is the Namibian continental slope. The region is influenced by the Benguela upwelling system that favours high productivity and the formation of organic–rich sediments. pH (Pfeifer et al., 2002) and therefore [CO_3^{2-}], within the topmost sediment layer are highly variable.

Oridorsalis umbonatus is an endobenthic foraminifer that lives in the uppermost centimetre of the sediment (Corliss, 1985; Rathburn and Corliss, 1994; Schmiedl et al., 1997). Due to its wide distribution it is used in paleoceanographic studies, particularly where *Cibicidoides* spp. is absent (e.g. Lear et al., 2000).

In a recent calibration study Rathmann et al. (2004) investigated the temperature–Mg/Ca relationship in *O. umbonatus* from the Namibian continental slope. Most of their samples were derived from water depth shallower than 1000m, where the steep temperature gradient towards the upper slope dominates any potential influence of [CO_3^{2-}]. However, the Mg/Ca from the deepest sample (2300m) in Rathmann et al. (2004) is – albeit only slightly – too high to be entirely temperature-controlled, suggesting the existence of an additional factor influencing shell composition.

In this study we investigate the relationships of Mg/Ca, Sr/Ca, $\delta^{13}C$, and $\delta^{18}O$ in the shell of *Oridorsalis umbonatus* with bottom- and pore-water [CO_3^{2-}] and $\Delta[CO_3^{2-}]$.

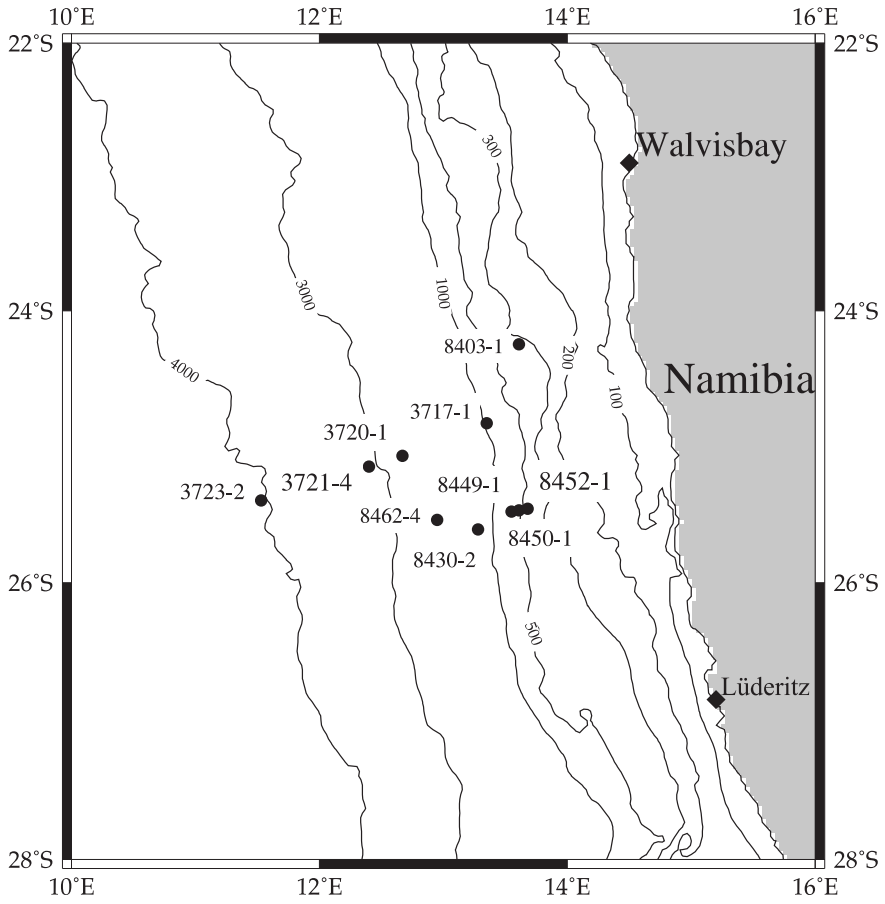

Figure 3.1.: Sample location and isobaths of the working area.

Our samples were retrieved from the Namibian continental slope over the depth range from 320 to 4000m; for water depth below 600m pore-water measurements have been available to us.

3.2. Material and Methods

3.2.1. Sampling

During METEOR cruises M34/2 and M57/2 (Schulz and cruise participants, 1996; Zabel and cruise participants, 2003) multicorers from the sediments underlying the Benguela upwelling system off Namibia were collected from water depths between 320 to 4000m. For the present study samples are used from ten stations (Table 3.1, Figure 3.1), including those from Rathmann et al. (2004). The sediments (mostly nannofossil ooze) were cut into 1cm slices immediately upon recovery and were preserved and stained with an ethanol/Rose Bengal solution. After washing the samples over a 125μm and a 63μm sieve, they were dried at 50°C. Out of the topmost cm five to ten individuals of *O. umbonatus* with a diameter of $300-400\mu$m were collected for measurements. Only well preserved tests, with all chambers were used.

A conductivity-temperature-depth logger (CTD SBE 911+) (Moorholz and Heene, 2003a) was deployed on each multicorer position on cruise M57/2. The measured

bottom water temperatures (BWT) at the investigated sites range from 2.9°C to 10.4°C (Table 3.1).

3.2.2. Trace elements

We used a Finnigan Laserprobe UV (266nm wavelength) laser ablation system, coupled to a ThermoFinnigan Element 2 sector field ICP-MS for the trace element analyses. The calibrations are based on the NIST610 glass standard reference material (SRM), assuming the composition according to Pearce et al. (1997).

We follow the procedures described in Rathmann et al. (2004) to determine elemental concentrations on the isotopes ^{25}Mg, ^{43}Ca and ^{88}Sr, where Ca was used as internal standard (assuming a Ca concentration of $40.04\%wt$). Errors in the assumed Ca content can lead to errors in the estimate of the absolute Mg and Sr content in the shell, but not in the calculated ratios. For this reason, we report the latter. As indicators for contaminants ^{55}Mn and ^{64}Zn were measured. The high energy density and the long acquisition time resulted in regular penetrations of the foraminiferal tests on one side. However, measurements of Zn, which is present in the adhesive tape that was used as sample holder, indicate that the duration of the ablation process was not sufficient to entirely penetrate the foraminiferal shell on both sides. Mn is present in both, clay minerals and iron-manganese crusts. Major contributions of contaminants were avoided by carefully selecting the time-resolved sample signal in each measurement run (see Rathmann et al., 2004). Each foraminiferal test was measured five times on different positions using a beam diameter of 70μm. The NIST610 standard was measured before and after each foraminiferal test. For each sample location, the final Mg/Ca and Sr/Ca ratios were calculated by averaging $25-50$ measurements (5 points per specimen, $5-10$ specimens per sample). Data points outside the 2σ range of the average were excluded. This procedure makes up for the high within- and between-shell variability for Mg/Ca (Rathmann et al., 2004). Standard errors of the averages range from 0.1 to 0.4mmol/mol for Mg/Ca, and from 0.01 to 0.03mmol/mol for Sr/Ca. To identify potential methodological biases of the laser ablation technique we measured the JCp-1 coral powder standard (Okai et al., 2002). Mg/Ca and Sr/Ca are systematically lower by 10 and 13%, respectively, than the values reported by Okai et al. (2002). No correction has been applied to the data reported in this study.

3.2.3. Stable isotopes

After laser ablation the test were analyzed for stable isotopes. $\delta^{13}C$ and $\delta^{18}O$ were determined using a Finnigan MAT 251 mass spectrometer equipped with an automated carbonate device. The analytical errors (1σ) are 0.07 for $\delta^{18}O$ and 0.03 for $\delta^{13}C$. The reproducibilities based on a laboratory standard calibrated against NBS 19 are < 0.07 for $\delta^{18}O$ and < 0.05 for $\delta^{13}C$.

Table 3.1.: Sample position, water depth, bottom water temperature, trace element ratios and stable isotopes of the tests of *Oridorsalis umbonatus* and stable isotopes of the seawater

MUC	lat. (°S)	long. (°E)	depth (m)	BWT (°C)	Mg/Ca ($\frac{\text{mmol}}{\text{mol}}$)	standard error	Sr/Ca ($\frac{\text{mmol}}{\text{mol}}$)	standard error	$\delta^{13}C$	$\delta^{18}O$	$\delta^{13}C_{sw}$	$\delta^{18}O_{sw}$
									(‰ VPDB)			
8403-1	24.25	13.61	320	10.41	3.962	0.181	1.046	0.010	-0.44	1.72	0.88	-0.06
8452-1	25.46	13.68	388	8.43	3.312	0.126	1.041	0.009	-0.47	2.11	0.90	-0.14
8450-1	25.47	13.61	506	6.42	2.497	0.095	0.990	0.006	-0.48	2.30	0.86	-0.16
8449-1	25.48	13.55	605	5.52	2.694	0.109	1.003	0.008	-0.73	2.30	0.81	-0.17
3717-1	24.83	13.35	855	3.93	2.180	0.100	0.961	0.006	-1.08	2.74	0.74	-0.19
8430-2	25.61	13.28	1330	3.33	1.908	0.082	0.965	0.009	-1.17	3.01	0.84	-0.13
8462-4	25.54	12.95	2293	2.91	2.138	0.212	0.890	0.009	-1.32	3.12	0.95	-0.06
3720-1	25.07	12.67	2516	2.87	2.338	0.200	0.906	0.014	-1.09	3.29	0.97	-0.07
3721-4	25.15	12.40	3014	2.55	2.758	0.411	0.954	0.030	-0.99	3.30	0.99	-0.07
3723-2	25.40	11.53	4004	1.62	1.719	0.100	0.878	0.032	-1.21	3.14	1.00[a]	-0.27[b]

[a] Mulitza et al. (1999, Figure 1b)
[b] Paul et al. (1999, Figure 8a)

3.2.4. Water samples

On cruise M57/2, water samples were taken from a depth of 3000m. Sample GeoB 84121-1 is from a transect at 23°S off Walvis Bay (Mulitza and Paul, 2003). The water samples for $\delta^{13}C$ were poisoned with mercury chloride and both (for $\delta^{13}C$ and $\delta^{18}O$) were sealed with paraffin immediately after recovery, and measurements for $\delta^{13}C$ and $\delta^{18}O$ were carried out using a Finnigan MAT Gasbench II system and an equilibration device connected to a Finnigan Delta S, respectively, at the Alfred-Wegener-Institut (AWI), Bremerhaven (Mackensen, unpublished data).The analytical errors are 0.03 for $\delta^{18}O$ equilibration and 0.07 for $\delta^{13}C$ gas bench.

3.2.5. Geochemistry of the pore-water

Geochemical analyses of the pore-water was carried out onboard the research vessel by the geochemistry group of the Geosciences Department of Bremen University directly after recovery to prevent sample alteration. Pore-water samples were squeezed from the same or parallel multicorer as the foraminifer samples (see Table 3.2). Titration with 0.01, 0.05 or $0.1M$ HCl was used to determine alkalinity, and pH was measured with an electrode before the sediment structure was disturbed. The analytical errors are better than 3% for alkalinity and 0.05 for pH. Data were provided by C. Hensen (GeoB 17xx and 37xx, available at the WDC-Mare database) and M. Zabel (GeoB 84xx, personal communication, 2006). Measurements were performed at the sediment surface and at 3 or 7mm sediment depth (Table 3.2). Our study concentrates on the data from 3mm depth.

3.2.6. Calculation of pH and carbonate ion concentrations

For calculating the carbonate ion concentrations and pH of the ambient water we used the program CO2SYS version 12 (Lewis and Wallace, 1998, modified by G. Pelletier, available at http://www.ecy.wa.gov/programs/eap/models/) with the dissociation constants chosen according to Dickson (1990) and Roy et al. (1993; 1994; 1996). Input parameters included temperature, salinity, silicate and phosphorous from the World Ocean Atlas 2001 (Conkright et al., 2002). Alkalinity and total inorganic carbon were taken from the GLODAP data set (Key et al., 2004). For the gridded data sets the grid cell centered at 25.5°S and 11.5°E was chosen.

The carbonate ion concentrations of pore-water was calculated using CTD temperatures, salinities from Conkright et al. (2002), and onboard measurements of alkalinity and pH (see above). Salinities are from the grid cells centered at 25.5°S and 11.5°E for the deepest sample (4004m), and from the grid cell centered at 25.5°S and 12.5°E for all other samples (the latter cell is closer to the sampling locations, but does not contain data below 3500m depth).

The parameters $[CO_3^{2-}]$ and pH are mutually dependent. We primarily report $[CO_3^{2-}]$; the results for pH are qualitatively the same.

Table 3.2.: Sample identification and position, water depth, pH, alkalinity, $[CO_3^{2-}]$ and $\Delta[CO_3^{2-}]$

Sample (foraminifera)	Sample (geochemistry)	lat., °S	long., °E	depth, m	pH (sediment surface)	pH (sediment depth: 3mm)	alkalinity, $\frac{mmol(eq)}{l}$ (sediment surface)	alkalinity, $\frac{mmol(eq)}{l}$ (sediment depth: 3mm)	$[CO_3^{2-}]$, $\frac{\mu mol}{kg}$ (sediment surface)	$[CO_3^{2-}]$, $\frac{\mu mol}{kg}$ (sediment depth: 3mm)	$\Delta[CO_3^{2-}]$, $\frac{\mu mol}{kg}$ (sediment surface)	$\Delta[CO_3^{2-}]$, $\frac{\mu mol}{kg}$ (sediment depth: 3mm)
8403-1	–	24.25	13.61	320	–	–	–	–	–	–	–	–
8452-1	8493-2	25.46	13.68	388	–	–	2.74	2.60	–	–	–	–
8450-1	8492-2	25.47	13.61	506	–	–	2.71	2.70	–	–	–	–
8449-1	8449-1	25.48	13.55	605	7.49	7.26	2.45	2.52	30.65	18.84	-16.61	-28.41
3717-1	3717-2	24.83	13.35	855	7.49	7.36	2.47	3.10	30.13	28.21	-19.43	-21.35
8430-2	8447-1	25.61	13.28	1330	7.63	7.21	2.75	2.93	46.23	19.41	-8.29	-35.11
8462-4	8462-4	25.54	12.95	2293	7.89	7.42	2.77	2.91	86.76	32.38	20.68	-33.71
3720-1	–	25.07	12.67	2516	–	–	–	–	–	–	–	–
3721-4	3721-4	25.15	12.40	3014	7.68	7.40	2.49	2.67	51.07	29.48	-25.22	-46.82
3723-2	1722-2[a]	25.40	11.53	4004	7.86	7.57	2.54	2.57	78.82	42.21	-13.61	-50.21

[a] Position is 2° north.

3.3. Results

3.3.1. Seawater

The bottom water temperature for the sampling locations ranges from about $10°C$ at $320m$ depth to about $1.5°C$ at $4000m$ depth (Figure 3.2 and Table 3.1), a change of $8.5°C$. Water column CO_3^{2-} and $\Delta[CO_3^{2-}]$ decrease significantly from the surface to a local minimum in the core of the Antarctic Intermediate Water in $800 - 1000m$ depth. Changes further down the water column are comparatively small, although [CO_3^{2-}] shows a minor local maximum at about $2500m$ within the North Atlantic Deep Water (NADW).

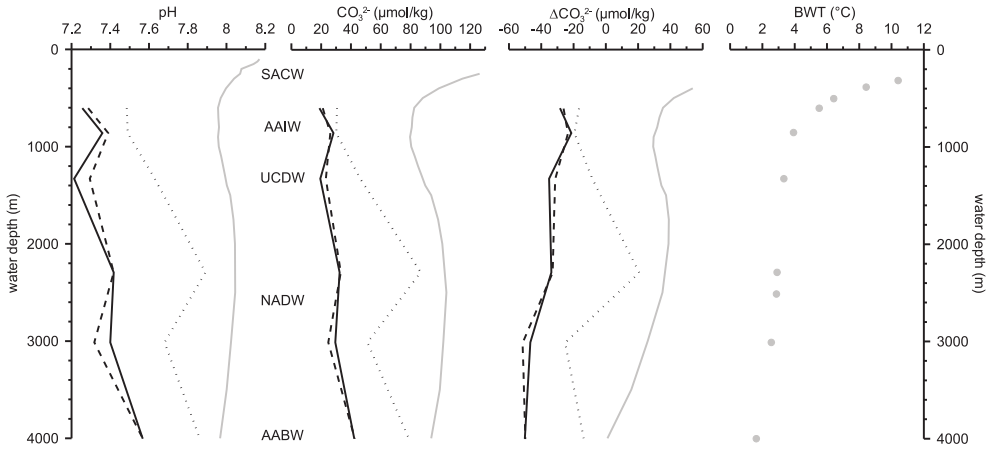

Figure 3.2.: Properties of the pore water and the water column. Water column measurements are in grey. pH, CO_3^{2-} and $\Delta[CO_3^{2-}]$ were calculated from the Glodap-Dataset (Key et al., 2004) and the WOA (Conkright et al., 2002; Stephens et al., 2002), BWT (grey points) are from the WOA (Stephens et al., 2002) and ship-board measurements. Pore-water measurements from the geochemical group at the geosciences department of Bremen University are marked in black. Dotted line: sediment surface; solid line: $3mm$ core depth; dashed line: $7mm$ core depth (Hensen et al., 1998, 2000; Zabel and cruise participants, 2003). SACW: South Atlantic Central Water, AAIW: Antarctic Intermediate Water, UCDW: Upper Circumpolar Deep Water, NADW: North Atlantic Deep Water, AABW: Antarctic Bottom Water.

Above $1000m$, CO_3^{2-} and $\Delta[CO_3^{2-}]$ strongly correlate with temperature. In cases where temperature exerts an influence on the shell composition this obscures the potential influences of the carbonate system parameters. However, most samples were recovered from depths greater than $1000m$, where temperature changes little, and the correlation between temperature, and CO_3^{2-} and $\Delta[CO_3^{2-}]$ is less pronounced. For $\delta^{18}O$ and Mg/Ca the effect of temperature can be quantified and subtracted (see below).

3.3.2. Pore water

Pore-water CO_3^{2-} and $\Delta[CO_3^{2-}]$ show generally increasing trends with water depth, although there is considerable scatter. A steep decrease is evident within the uppermost millimeters of the sediment for each site, but this has little effect on the aforementioned trend between sites (Figure 3.2, Table 3.2).

Interestingly, there are no similarities between the data from the water column and the sediment pore-water chemistry, and trends with water depth are even opposed, suggesting that ocean and pore-water chemistry off Namibia are largely independent.

Comparing shell composition with pore-water chemistry is complicated by the fact that pore-water chemistry changes significantly within the upper few centimeters of the sediment, whereas the exact depth habitat of the individual foraminifera is unknown. However, $[CO_3^{2-}]$ changes at approximately the same rate versus sediment depth at most coring sites. Provided that the preferred calcification depth within the sediment of *O. umbonatus* does not vary systematically between sites, this means that linear relationships (if present) between $[CO_3^{2-}]$ and shell composition will retain their gradients independent of the sediment depth that $[CO_3^{2-}]$ were derived from. However, systematic offsets are possible, which should be considered for the next sections.

3.3.3. Sr/Ca

Shell Sr/Ca shows a roughly linear decrease with depth from 1.05mmol/mol at 320m to 0.88mmol/mol at 4000m. There is a statistically significant linear relationship with BWT ($\mathrm{Sr/Ca} = 0.87 + 0.02 * \mathrm{BWT}; \mathrm{R}^2 = 0.81$). However, the regression is entirely based on the linear trends in both parameters, and no correlation exists for the detrended data sets. This suggests that the decrease in Sr/Ca with depth is not necessarily temperature-driven. As for Mg/Ca a local maximum is present in Sr/Ca at 3000m depth, that it not accompanied by a comparable change in the bottom water properties.

The comparison of Sr/Ca with pore-water $[CO_3^{2-}]$ and $\Delta[CO_3^{2-}]$ (Figures 3.3a and 3.5a) reveals significant linear relationships ($\mathrm{Sr/Ca} = 1.03 + 0.002 * \Delta[CO_3^{2-}], \mathrm{R}^2 = 0.29; \mathrm{Sr/Ca} = 1.08 - 0.005 * [CO_3^{2-}], \mathrm{R}^2 = 0.8$; see Table 3.3). The correlations are not only based on the linear trends with water depth, but also on the residual variability after the trend is removed. This strongly suggests that shell Sr/Ca in *O. umbonatus* is a function of the carbonate system parameters of the ambient pore-water.

3.3.4. Mg/Ca

Mg/Ca generally decreases with increasing water depth from ~ 4mmol/mol at 320m to 1.7mmol/mol at 4000m (Figure 3.3b and Table 3.1). In the shallower stations down to 1330m the decreasing Mg/Ca trend closely follows the decrease in water temperature. However, at greater depth, a notable local maximum is present at 3000m. This anomaly is not related to bottom water temperatures or any other physical parameters of the water column. This anomaly is also evident when Mg/Ca is plotted as function of temperature (Figure 3.4). Most data points fall close to the expected exponential fit, except for the samples recovered between 2300m and 3000m water depth.

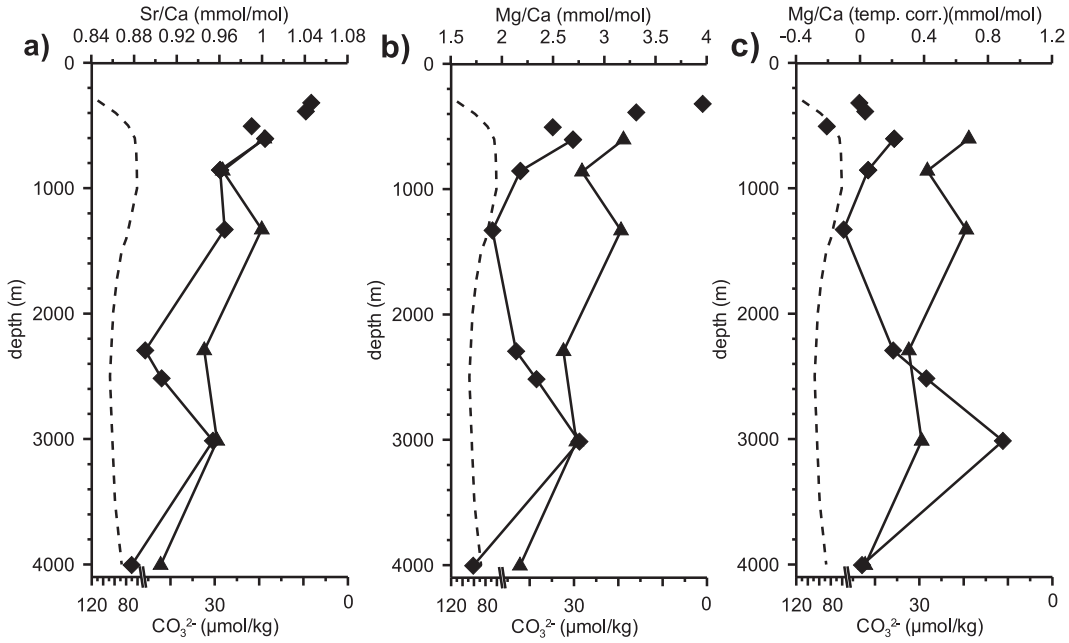

Figure 3.3.: Sr/Ca (a), Mg/Ca (b) and Mg/Ca (temp. corr.)(c) profile (solid line with diamonds). Dashed lines indicate $[CO_3^{2-}]$ from the water column. Solid line with triangles indicate CO_3^{2-} from the pore-water (3mm core depth).

While the local Mg/Ca maximum at 3000m does not correlate with water column properties, it does correspond to a local minimum in $[CO_3^{2-}]$ and $\Delta[CO_3^{2-}]$ of the pore-water. This suggests that the pore-water carbonate system influences the shell Mg/Ca. Since a potential relationship is obscured by the influence of temperature on Mg/Ca for the shallower part of the profile, we calculated temperature corrected Mg/Ca values (Mg/Ca_{corr}). Mg/Ca was calculated from BWT by applying the calibration of Rathmann et al. (2004) and subtracting the result from measured Mg/Ca (Figure 3.3c). However, apart from the 3000m anomaly, there is little resemblance between the Mg/Ca_{corr} and the pore-water chemistry, which is evident in the low correlations (Figures 3.3b and 3.5b, Tables 3.1 and 3.2).

In contrast to Sr/Ca, Mg/Ca scatters significantly between individual ablation points from the same shell, the standard deviation is about 0.15. The distribution pattern is random, there is no relationship with the position within or between chambers nor did we observe ontogenetic trends.

3.3.5. Carbon isotopes

$\delta^{13}C$ decreases from -0.4‰ at 320m to -1.3‰ at 2300m water depth (Figure 3.6a). A broad excursion back towards heavier values characterizes the deeper part of the profile. As for Mg/Ca and Sr/Ca a local maximum exists at 3000m depth (Table 3.1). There is no similarity between the profiles of shell $\delta^{13}C$ and any of the bottom water parameters, and even between shell $\delta^{13}C$ and $\delta^{13}C_{sw}$.

The comparison of shell $\delta^{13}C$ with pore-water chemistry (Figures 3.6a, 3.5c) suggests a weak negative correlations with $\Delta[CO_3^{2-}]$ and $[CO_3^{2-}]$, although these are not

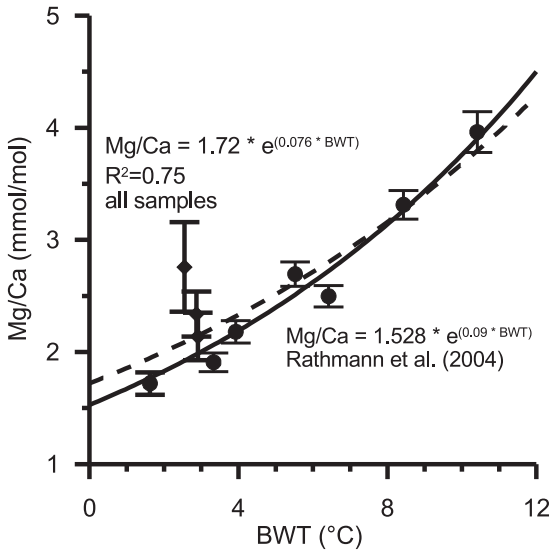

Figure 3.4.: Comparison of mean Mg/Ca ratios of *O. umbonatus* of our data with data from Rathmann et al. (2004)(solid line). Vertical bars indicate standard errors of all measurements from core top sample. BWT has been derived from local CTD measurements at the sampling positions and from the WOA (Stephens et al., 2002)). Formula calculated from all mean values (dashed line).

statistically significant. The influence of temperature on carbonate $\delta^{13}C$ is a matter of debate (Romanek et al., 1992; Russell and Spero, 2000). If $\delta^{13}C$ is corrected for $\delta^{13}C_{sw}$ and/or temperature the general shape of the $\delta^{13}C$ curve with water depth (Figure 3.6a) changes slightly, but the correlations with $\Delta[CO_3^{2-}]$ and $[CO_3^{2-}]$ to remain insignificant (Table 3.3).

3.3.6. Oxygen isotopes

$\delta^{18}O$ values range from 1.7‰ at 320m to 3.3‰ at 3000m depth (Figure 3.6b). The $\delta^{18}O$ profile matches that of temperature without major deviations. To assess the potential impact of sea- and pore-water chemistry we subtracted the temperature component from the measured $\delta^{18}O$ data by applying the calibration of Shackleton (1974). We also subtracted the $\delta^{18}O$ of seawater, although the potential impact on the overall variability of shell $\delta^{18}O$ is small given the range of $\delta^{18}O_{sw}$ of only 0.12‰. We will subsequently use the term $\delta^{18}O_{corr}$ for the corrected shell $\delta^{18}O$. When the deepest sample (4000m) is excluded, $\delta^{18}O_{corr}$ shows little variability (Figure 3.6c), often only marginally exceeding the analytical uncertainty. There is no discernible trend with water depth. A correlation with pore-water $[CO_3^{2-}]$ is evident, but this relationship should be viewed cautiously given the analytical limits.

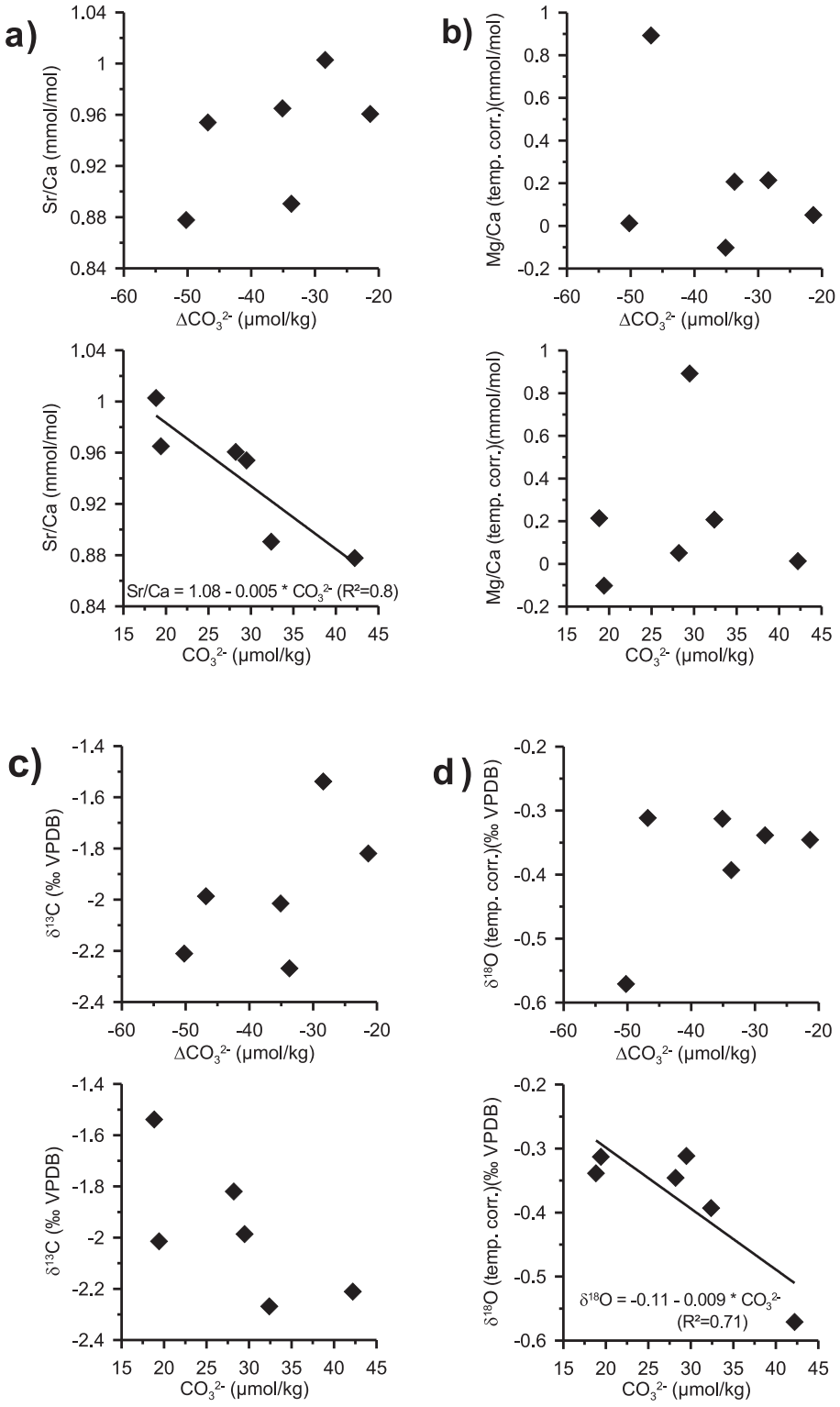

Figure 3.5.: Sr/Ca (a), Mg/Ca (temp. corr.) (b), $\delta^{13}C$ (corr. for seawater) (c) and $\delta^{18}O$ (temp. corr.) (d) against ΔCO_3^{2-} and CO_3^{2-}.

Table 3.3.: Relationsships between environmental and shell geochemical parameters

Environmental Parameter	Geochemical Parameter	Equation	R^2	n	$p <$
BWT	Sr/Ca	$\mathrm{Sr/Ca} = 0.87 + 0.02 * \mathrm{BWT}$	0.81	10	0.01
BWT	Mg/Ca	$\mathrm{Mg/Ca} = 1.528 * exp(0.09 * \mathrm{BWT})^a$	0.93[a]		
pH	Sr/Ca	$\mathrm{Sr/Ca} = 3.30 - 0.32 * \mathrm{pH}$	0.71	6	0.05
CO_3^{2-}	Sr/Ca	$\mathrm{Sr/Ca} = 1.08 - 0.005 * CO_3^{2-}$	0.80	6	0.05
$\Delta[CO_3^{2-}]$	Sr/Ca		0.29	6	n.s.
pH	Mg/Ca (temp. corr.)		0.02	6	n.s.
CO_3^{2-}	Mg/Ca (temp.corr.)		0.00	6	n.s.
$\Delta[CO_3^{2-}]$	Mg/Ca (temp.corr.)		0.14	6	n.s.
pH	$\delta^{13}C$		0.21	6	n.s.
CO_3^{2-}	$\delta^{13}C$		0.33	6	n.s.
$\Delta[CO_3^{2-}]$	$\delta^{13}C$		0.07	6	n.s.
pH	$\delta^{13}C$ (corr. for seawater)		0.39	6	n.s.
CO_3^{2-}	$\delta^{13}C$ (corr. for seawater)		0.50	6	n.s.
$\Delta[CO_3^{2-}]$	$\delta^{13}C$ (corr. for seawater)		0.33	6	n.s.
pH	$\delta^{13}C$ (corr. for seawater and BWT)		0.07	6	n.s.
CO_3^{2-}	$\delta^{13}C$ (corr. for seawater and BWT)		0.02	6	n.s.
$\Delta[CO_3^{2-}]$	$\delta^{13}C$ (corr. for seawater and BWT)		0.02	6	n.s.
pH	$\delta^{18}O$ (corr. for seawater and BWT)	$(\delta^{18}O = 4.41 - 0.65 * \mathrm{pH})^b$	0.69	6	0.05
CO_3^{2-}	$\delta^{18}O$ (corr. for seawater and BWT)	$(\delta^{18}O = -0.11 - 0.009 * CO_3^{2-})^b$	0.71	6	0.05
$\Delta[CO_3^{2-}]$	$\delta^{18}O$ (corr. for seawater and BWT)		0.27	6	n.s.

Note: for pH and CO_3^{2-} only the slope is meaningful. The validity of the offset depends on the actual habitat depth of *O. umbonatus* within the sediment. See text for details.
p is the propability that the parameters are uncorrelated (two-tailed t-test).
n. s. = non-significant
[a] Rathmann et al. (2004)
[b] For $\delta^{18}O$ the variability is close to the analytical error.

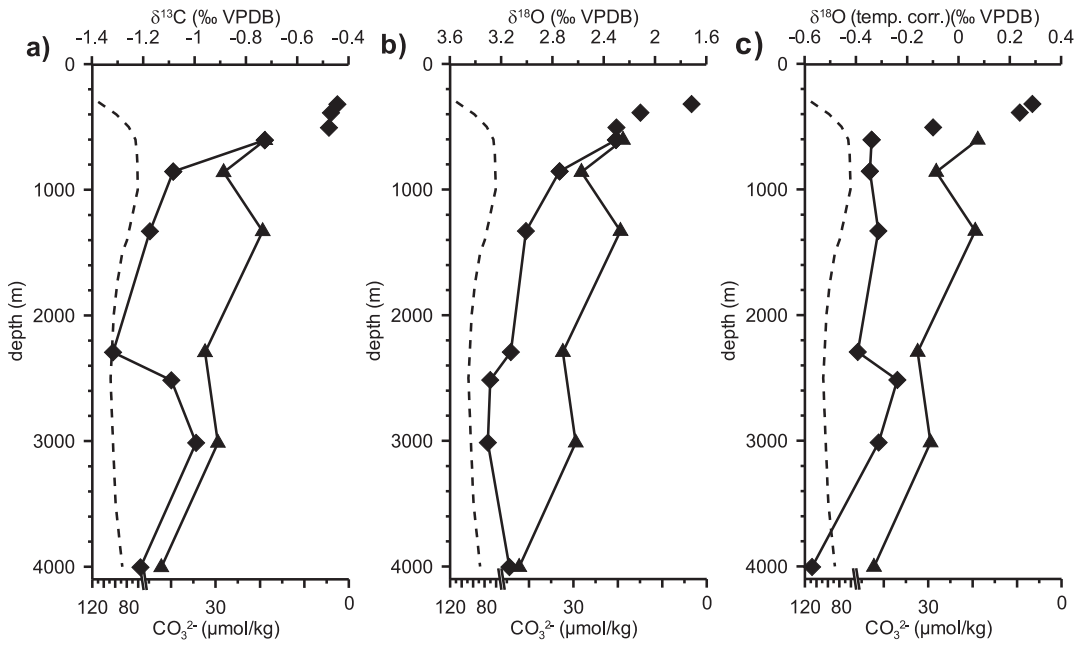

Figure 3.6.: $\delta^{13}C$ (a), $\delta^{18}O$ (b) and $\delta^{18}O$ (temp. corr.)(c) profile (solid line with diamonds). Dashed lines indicate $[CO_3^{2-}]$ from the water column. Solid line with triangles indicate CO_3^{2-} from the pore-water (3mm core depth).

3.4. Discussion

3.4.1. Dissolution

Partial dissolution of shell material can significantly alter the chemical composition due to selective leaching of Mg and Sr (McCorkle et al., 1995; Brown and Elderfield, 1996; Fehrenbacher et al., 2006). Since the pore-water at our sampling sites is often corrosive, dissolution is a potential problem. However, in case of dissolution we would expect a positive correlation between the element:Ca ratios and $[CO_3^{2-}]$ (low $[CO_3^{2-}]$ is indicative of corrosive water, where leaching of Sr and Mg should be strongest). This is not the case, and we conclude that dissolution does not pose a major problem in our samples.

3.4.2. Sr/Ca

The Sr/Ca values decrease with increasing water depth. However, no clear temperature dependency can be inferred. Similar results have been reported for both benthic and planktonic species (Rosenthal et al., 1997). Although an influence of temperature on foraminiferal Sr/Ca cannot be ruled out (Mortyn et al., 2005), the overall importance is small. This is in line with Sr/Ca in high-Mg calcitic ostracodes (De Deckker et al., 1999), but contrasts with aragonitic corals (Beck et al., 1992; Alibert and McCulloch, 1997; Felis et al., 2004), where temperature exerts a dominant control. The interpretation of the role of temperature is further complicated by inconsistent results from inorganic calcite precipitation experiments. The temperature dependency of Sr/Ca

ranges from positive (Malone and Baker, 1999) to insignificant (Katz et al., 1972) to negative (Kinsman, 1969).

Sr/Ca of seawater varies between ocean basins and with water depth (Bernstein et al., 1987; de Villiers, 1999). Unless major carbonate dissolution takes place within the sediment this would affect both bottom and pore-water. However, the variability for the South Atlantic (de Villiers, 1999) is only about 5% of the mean, while it is 17% for the foraminiferal shells. We therefore exclude water Sr/Ca as the primary driver of shell Sr/Ca, although it may represent a secondary modifier.

A significant influence of pore-water [CO_3^{2-}] on shell Sr/Ca is evident, a change in [CO_3^{2-}] of 10μmol/kg results in a change in Sr/Ca of -0.05mmol/mol (Figure 3.3a). The absolute variability of Sr/Ca between samples is small, but approximately 90% can be explained by changes in [CO_3^{2-}]. In contrast to [CO_3^{2-}] the influence of $\Delta[CO_3^{2-}]$ is marginal ($\sim 8\%$).

Interestingly, the negative correlation of Sr/Ca and [CO_3^{2-}] for *O. umbonatus* is opposed to that for *Orbulina universa* (Russell et al., 2004) and *Hoeglundina elegans* (Rosenthal et al., 2006), where the correlations are positive. The results also differ from those for *Globigerina bulloides*, where no significant relationship exists (Russell et al., 2004). This indicates that the influence of [CO_3^{2-}] on foraminiferal Sr/Ca is strongly species-specific. *Orbulina universa* is symbiotic and *H. elegans* is aragonitic, which suggests a potential role of endosymbionts and shell mineralogy on the sign of the Sr/Ca versus [CO_3^{2-}] relationship.

3.4.3. Mg/Ca

As indicated previously the expected dependency of foraminiferal Mg/Ca ratios from the ambient bottom water temperature is clearly present, where the Mg/Ca ratios fall close to the calibrations of Rathmann et al. (2004) and Lear et al. (2002), where the latter is based on independent data.

The positive excursion between 2293m and 3014m water depth in both Mg/Ca and Mg/Ca_{corr} coincides with a negative excursion in pore-water [CO_3^{2-}]. Following previous studies on planktonic foraminifera (Lea et al., 1999; Russell et al., 2004) the decrease in pore-water [CO_3^{2-}] by 10μmol/kg from 2300m to 3000m water depth should result in a Mg/Ca increase of about $0.3-0.5$mmol/mol, which compares with a change in Mg/Ca of 0.3 per 10μmol/kg [CO_3^{2-}] decrease in our data (Table 3.3). Although this excursion in Mg/Ca may be explained by changes in [CO_3^{2-}], the data from shallower water do not support a general [CO_3^{2-}]–dependency of Mg/Ca, which is evident by the lack of coincidence with Mg/Ca_{corr} (Figure 3.3c). Russell et al. (2004) have shown that pH and [CO_3^{2-}] only impact the shell Mg concentration below thresholds of pH 8.2 and [CO_3^{2-}] of 200μmol/kg of the ambient water under laboratory conditions. The pore-water at our sampling sites is often under-saturated with respect to calcite, and [CO_3^{2-}] remains well below the above values, suggesting that the "threshold effect" is not present here. Elderfield et al. (2006) compared Mg/Ca in *C. wuellerstorfi* with bottom water $\Delta[CO_3^{2-}]$ on a global scale, where the Atlantic was the only ocean without significant relationship. In essence, a high proportion of the Mg/Ca variability (sometimes more than one third) in *O. umbonatus* remains unexplained below temperatures of ~ 4°C.

The variability in Mg/Ca within shells of *O. umbonatus* from the same sediment

sample suggests that Mg is not homogeneously distributed. Within-shell variability along the shell surface or between shell layers has been previously ascribed to temperature changes during growth (Toyofuku et al., 2000; Eggins et al., 2004), ontogenetic trend (Anand and Elderfield, 2005; Toyofuku and Kitazato, 2005), and variations that have no apparent dependency on ontogenetic or environmental parameters (Hathorne et al., 2003; Eggins et al., 2003, 2004). We can exclude the first two possibilities, since temperature variability at the sampling sites is small, and no ontogenetic trends have been observed. Alternatively, changes in the ambient [CO_3^{2-}], e.g., due to vertical migration of the foraminifer, could induce changes in the shell Mg/Ca. The problem with this explanation is that we would expect a similar magnitude of variability in Sr/Ca, where the dependency on [CO_3^{2-}] is significant (see above). Although the intra-shell variability for Mg/Ca is high and the exact reason remains enigmatic, the impact on the average calculated for each sediment sample remains relatively small.

3.4.4. Carbon isotopes

The dependence of foraminiferal $\delta^{13}C$ from [CO_3^{2-}] has been previously demonstrated in both culturing experiments and samples from plankton tows (Spero et al., 1997; Bauch et al., 2002; Wilke et al., 2006). The likely reason for the lack of a clear correlation in the Namibian samples is the unknown value of pore-water $\delta^{13}C$, which may differ from bottom water $\delta^{13}C$. Generally, the oxidation of organic matter in the sediment releases ^{13}C–depleted carbon resulting in the drop of pore-water $\delta^{13}C$. Therefore, the $\delta^{13}C_{shell}$ is often influenced by the flux of organic matter to the sediment (Zahn et al., 1986; Mackensen and Bickert, 1999), leading to offsets of up to -0.6‰ in extreme cases.

3.4.5. Oxygen isotopes

The gradient in $\delta^{18}O_{corr}$ versus pore-water [CO_3^{2-}] is higher but of the same order of magnitude compared to the results of culturing studies of planktonic species by Spero et al. (1997) and Zeebe (1999), and inorganic calcite precipitation experiments (McCrea, 1950). To some extent the difference in the slope may be caused by the issue outlined in the Results section. However, it is likely that species-specific effects contribute to the difference. Even among the (planktonic) species studied so far the slope ranges between 0.002‰ $\delta^{18}O$ / μmol/kg [CO_3^{2-}] for *Orbulina universa* and 0.005 for *Globigerina bulloides* (Spero et al., 1997), while no influence of [CO_3^{2-}] on $\delta^{18}O$ has been found for *Globorotalia inflata* (Wilke et al., 2006).

Theoretically, [CO_3^{2-}] should exert a stronger influence on endobenthic compared to epibenthic species given the variable composition of pore-water. There are currently no systematic comparisons that include direct measurements of pore-water [CO_3^{2-}]. Results purely based on $\delta^{18}O$ are ambiguous: for example, there is no difference between the epibenthic *Cibicidoides wuellerstorfi* and the endobenthic *C. kullenbergi* (McCorkle et al., 1990), but Mulitza and Paul (2003) suggested that the 0.6‰ offset between *C. wuellerstorfi* and the endobenthic *Uvigerina peregrina* may be due to different carbonate ion concentrations in the ambient water. However, due to the absence of [CO_3^{2-}] data there is no clear distinction between the influences of [CO_3^{2-}] and vital effects.

3.4.6. Influence of water masses

Variations in water mass properties have been previously suggested to influence the foraminiferal shell chemistry (Martin et al., 1999). Our sampling transect penetrates some of the major water masses of the South Atlantic. With respect to the carbonate system, the strongest contrast exists between the high-[CO_3^{2-}] NADW on one hand and the highly corrosive, low-[CO_3^{2-}] AAIW and AABW on the other hand (Figure 3.2). The anomalies in our Mg/Ca, Sr/Ca, and $\delta^{13}C$ data are centred at about 3000m depth, which would correspond to the NADW. While at first this hints at a potential water mass effect, the closer inspection of the water column chemistry reveals that there is no change equivalent to the anomaly in the shell composition. Furthermore, the local extremes in water chemistry that characterizes the AAIW core (at around 800m) are not accompanied by anomalies or local extremes in our geochemical data. This lack of coincidence is not surprising, given the degree of independence between the pore-water and the water column. Together with the clear influence of the pore-water on shell Sr/Ca and $\delta^{13}C$, this demonstrates that *O. umbonatus* off Namibia records pore-water, not water column, properties.

3.5. Conclusions

We measure trace element and stable isotope ratios in *O. umbonatus* and compared the results with the chemical and physical properties of the water column and the pore-water. Only the latter appeared to influence the shell composition. We observe a negative correlation between $\delta^{18}O_{corr}$ and [CO_3^{2-}], which is expected from previous observations and experiments. The variability in $^{18}O_{corr}$ between the sample stations is small, and we suggest further investigation covering a broader range of values.

A significant [CO_3^{2-}]–dependence was inferred for Sr/Ca, in fact, most of the Sr/Ca variability can be attributed to changes in [CO_3^{2-}]. In contrast to previous studies, the sign of the relationship is negative. Nevertheless, the results indicate that Sr/Ca in *O. umbonatus* offers the potential as a paleo-proxy for pore-water [CO_3^{2-}] in future studies. Generally, the influence of [CO_3^{2-}] rather than $\Delta[CO_3^{2-}]$ appears more important. No clear influence was observed for $\delta^{13}C$ and Mg/Ca.

The results indicate that it is important to distinguish between the chemical properties of pore-water and the water column. At least for organic-rich sediments it is necessary to use pore-water measurements to investigate the influence of the carbonate system on the shell composition in endobenthic foraminifera.

Acknowledgements We thank Monika Segl and her team for the stable isotope measurements. Andreas Mackensen and André Paul provided water stable isotope data, Matthias Zabel made the pH data available, and Iris Wilke introduced us to the CO2SYS software. We thank Stefan Mulitza for discussions and many valuable suggestions, and Heather Johnstone for improving the English. Gert-Jan Reichart and an anonymous reviewer are thanked for their constructive and helpful comments. This work was funded by the Deutsche Forschungsgemeinschaft (DFG Research Center Ocean Margins Contribution No. RCOM0524).

Supplementary data Supplementary data associated with this article can be found, in the online version, at doi:10.1016/j.marmicro.2007.08.001 and in Chapter A.

4. Stratification of eastern South Atlantic (25°S) upper water masses during the Last Glacial Maximum

Söhnke Rathmann, Henning Kuhnert, André Paul, Oscar Romero and Stefan Mulitza
manuscript in preparation for submission to Geophysical Research Letters

Abstract We investigate the changes in the water mass stratification between the Holocene and the Last Glacial Maximum. Trace elements and stable isotopes were measured on *Oridorsalis umbonatus* of six multicores and six gravity cores to determine bottom water temperatures and salinity. The calculated density represent that our samples follow the water masses downslope in the regular sequence. Bottom water temperatures (BWT) show nearly no changes between the Last Glacial Maximum and modern values. Interestingly, in the shallow cores, which were most influenced, we observe slightly warmer BWTs during the LGM, which is in contrast to the findings of Niebler et al. (2003), who investigated inter alia nearby cores with a modified version of the Imbrie-Kipp-Tranfer-Function. These opposed changes between BWTs and sea surface temperatures (SST) suggest a movement of the water masses.

4.1. Introduction

The permanent thermoclines in the subtropical gyres constitute about 15%–20% of the World Ocean volume (Karstensen and Quadfasel, 2002). This volume is ventilated through subduction, which is the flux across the base of the mixed layer at mid- and low latitudes (Luyten et al., 1983). The waters in the thermocline store, transport and release heat and nutrients. Therefore thermocline processes exert primary control over the cycling and vertical distribution of nutrients and heat in the ocean (e.g. Slowey and Curry, 1995), and may act as a buffer or amplifier for changes in the earth's climate system. Furthermore, the associated thermocline circulation provides a route of communication between the midlatitudes and the tropics (e.g. Johnson and McPhaden, 1999). This is especially true for the upwelling regions offshore Southwest Africa where the characteristics of the local hydrography (and presumably that of the local productivity) seems to be highly dependent on the properties of the upwelled thermocline water (Niebler et al., 2003; Paul and Schäfer-Neth, 2003), which are preformed at higher latitudes.

The model results of the modelling group of the Geosciences Department at Bremen University yield strong evidence for a glacial shallowing of both mixed layer and

thermocline in the Namibian upwelling region. In concert with higher glacial wind speeds and increased upwelling velocity, this shallowing resulted in a more efficient vertical exchange between these two uppermost layers of the ocean. At the same time, the balance of Angola and Benguela Current was shifted towards the latter, which was dominated by the cold water preformed near Drake Passage (instead of Indian Ocean Waters).

In the western North Atlantic the glacial thermocline was also characterized by a cooler, shallower and more uniformly ventilated thermocline (Slowey and Curry, 1995). However, it is still unknown how this changed glacial thermocline structure affected the upwelling regions in the eastern North Atlantic off Northwest Africa.

The strength of the temperature decrease in the last glacial maximum (LGM) has been extensively discussed (e.g. CLIMAP-Project Members, 1981; Niebler et al., 2003, on a global scale and on a regional scale, respectively). Niebler et al. (2003) reconstructed a temperature difference of $10°C$ for the shallow area off Namibia. They used a modified version of the Imbrie-Kipp transfer function method to reconstruct sea-surface temperatures (SST) from foraminiferal faunal assemblages. The validation or refutation of these huge changes in temperature will be discussed here.

With the aid of Mg/Ca and $\delta^{18}O$ of the benthic foraminifera *Oridorsalis umbonatus* it is also possible to reconstruct the salinity. The Mg/Ca values were used to reconstruct the temperature, which is therefore independent from the stable oxygen isotopes and can be used in the well known equation from Epstein et al. (1953) to calculate the $\delta^{18}O$ of seawater ($\delta^{18}O_{sw}$). These $\delta^{18}O_{sw}$ is the variable to calculate the salinity (see Wolff et al., 1999).

Since a few years the influence of the carbonate ion concentration ($[CO_3^{2-}]$) on the incorporation of trace elements is discussed (e.g. Russell and Spero, 2000; Russell et al., 2004; Elderfield et al., 2006). In a recently published article, Rathmann and Kuhnert (2008) explored the influence of $[CO_3^{2-}]$ on the trace element ratios of *O. umbonatus*. They found only a sensitivity with Sr/Ca and $\delta^{18}O$. Therefore, the $[CO_3^{2-}]$ will be ignored, due to their small influence on Mg/Ca.

4.1.1. Regional Setting

Off Namibia, the surface layer is characterised by warm water of higher salinity originating from the northern Benguela. The SST increases offshore, and at the coast a very weak upwelling structure is found. Below the surface mixed layer oxygen depleted central water covers the entire shelf and the continental margin to $12.2°E$. The decomposition of organic matter caused anoxic conditions in the bottom layer at the shelf. The core of the Antarctic Intermediate Water (AAIW) was identified by the salinity minimum at 800m depth. The secondary salinity maximum near 2200m is associated with the North Atlantic Deep Water (NADW).

The thermocline water off Namibia consists of two different central water masses and their mixing stages. Saline, nutrient rich but oxygen depleted South Atlantic Central water (SACW) originating from the tropical ecosystem enters the Benguela system from the north. Fresher, nutrient-depleted and oxygen-rich Eastern South Atlantic Central Water (ESACW) is transported with the Benguela Current (BC) northward. In the upper central water layer ($13°C$ isotherm, ~ 150m depth, Moorholz and Heene, 2003b) the SACW reach to $24°S$ and covers only the shelf. The major portion of the

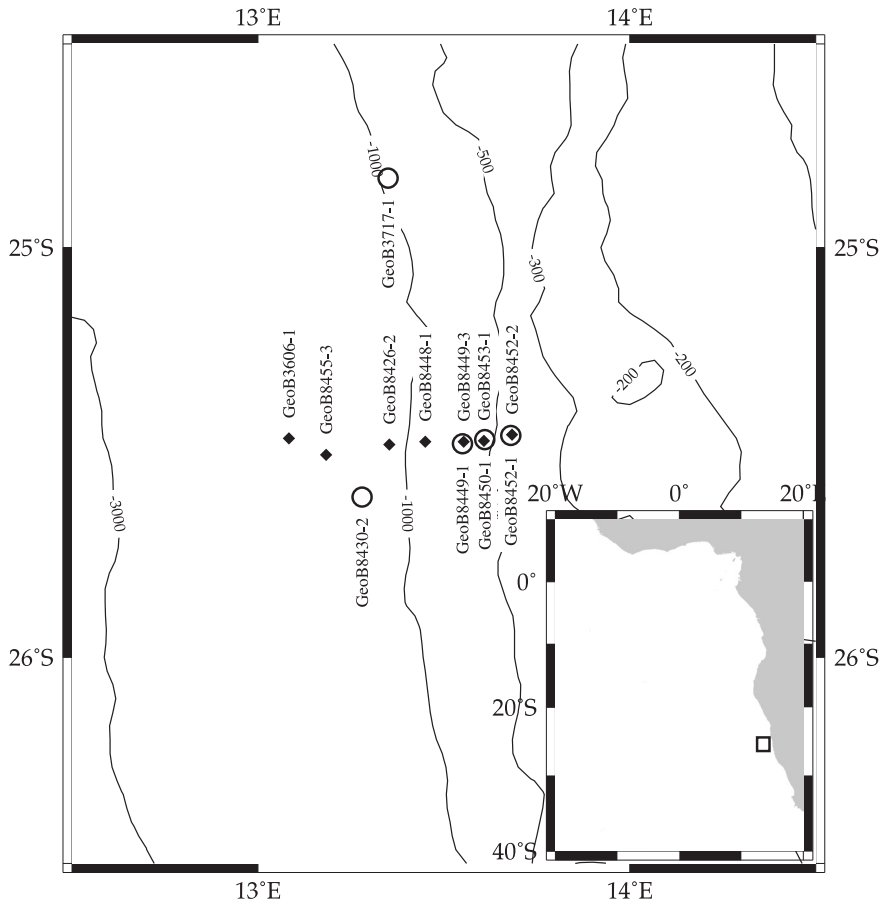

Figure 4.1.: Regional map with gravity core (filled diamonds, names above) and multicorer locations (open circles, names below, Rathmann et al. (2004); Rathmann and Kuhnert (2008)).

upwelled water at the coast originating from this depth. This causes a higher on shore transport of central water. In the deeper layers increase the southward extension of SACW at the shelf (see salinity distribution at the $10°$C isotherm, ~ 250m depth in Moorholz and Heene, 2003b). This may be caused by a higher intensity of the poleward undercurrent and a decreasing onshore transport of ESACW. Due to its different oxygen and nutrient content the distribution of central water play an important role for ventilation of the subsurface layer and the productivity of the Benguela upwelling system.

4.2. Methods

4.2.1. Core locations

For this study, samples from seven gravity cores and six multicorer cores from the Benguela upwelling system off Namibia was used. The cores are from a water depth range of $387 - 1785$m collected during METEOR cruise M57/2 (Zabel and cruise participants, 2003) and M34/1 (Bleil and cruise participants, 1996) (Figure 4.1). During the LGM sea level was ~ 120m lower (Fairbanks, 1989), hence the paleodepth

Table 4.1.: Conventional radiocarbon ages of three planktonic foraminiferal samples of core GeoB 8453-1.

Leibniz Laboratory identification	Sample depth, cm	Foraminiferal species	Conventional ^{14}C (yr BP)	Error (years)
KIA 25078	3	*G. bulloides*	9340	50
KIA 25076	168	*G. bulloides*	18280	100
KIA 27300	223-213	*G. bulloides* and *N. pachyderma*	32090	+810/-730

of the sampling sites ranged from ~ 270 to 1570m. Nowadays, the primary depth of the South Atlantic Central Water (SACW) lies at about $200 - 300$m. Underneath the SACW lies the Antarctic Intermediate Water (AAIW) up to the depth of 800m. The Upper Circumpolar Deep Water (UCDW, ≤ 1200m) and the North Atlantic Deep Water (NADW) until 2500m complete the water masses that influence the core locations. On board of R/V METEOR, the sediment core was split into two halves and syringe samples were taken every 5cm, beginning with 3cm core depth.

4.2.2. XRF

The XRF core scanner allows the non-destructive, nearly continuous, and relatively fast analysis of the elemental composition of the sediment cores, which we use to establish a common stratigraphy (see Section 4.2.3). Data are reported as element intensities in counts per second (cps), these are proportional to the elemental concentrations. Element intensities are additionally influenced by the energy level of the X-ray source, the count time, and the physical properties of the sediment (e.g. porosity). Down-core variations of physical properties can be an issue for analyses that are obtained directly at the split core surface (see Tjallingii et al., 2007). However, the measurements still provide qualitative information on changes in the elemental composition.

4.2.3. Stratigraphy

On gravity cores GeoB 3606-1 and GeoB 8453-1 AMS-^{14}C-datings were performed (see Romero et al. (2003, their Table 1) and Table 4.1). The datings for GeoB 8453-1 show, that the most recent $10,000$ years are lost. Additionally, all cores were investigated with XRF analysis and the Fe-data were used in this study to correlate the cores. In cores GeoB 3606-1 and GeoB 8453-1 the end of the LGM is characterized by high Fe-intensities followed by a marked decrease. This pattern has been used to identify the LGM in the other cores (shaded area in Figure 4.2).

4.2.4. Elemental composition and stable isotopes

The laser ablation technique, described in detail in Rathmann et al. (2004) and Rathmann and Kuhnert (2008), was used to determine the Mg/Ca-ratios of the benthic fo-

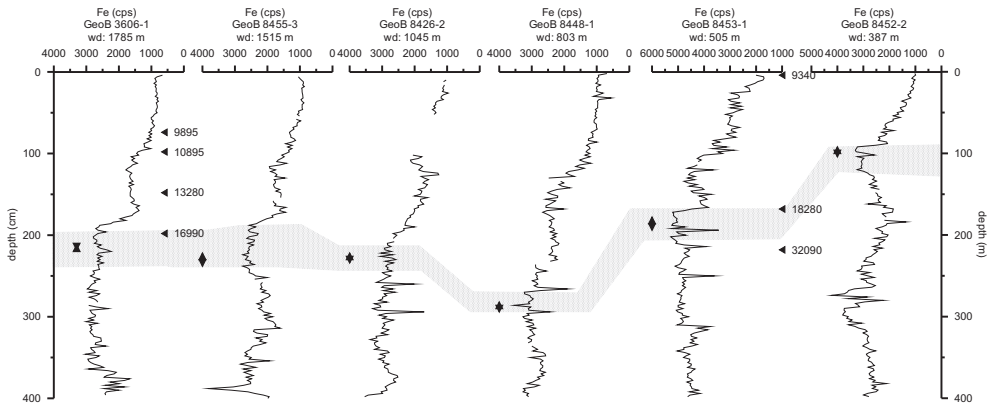

Figure 4.2.: XRF-Fe-measurements of the gravity cores to determine the LGM (shaded area). Arrows indicate the measurment range. Triangles indicate AMS-^{14}C measurements with uncalibrated ages.

raminifera *Oridorsalis umbonatus*. Measurements are based on the isotopes ^{25}Mg and ^{43}Ca. ^{55}Mn and ^{64}Zn were measured as indicators of contaminants. Mn is present in iron-manganese crusts, while Zn indicates the penetration of the shell and the ablation of the sample holder. Each foraminiferal test was measured five times on different positions using a beam diameter of 70μm. The NIST610 standard was measured before and after each foraminiferal test. For each sediment sample, the final Mg/Ca ratios were calculated by averaging $5 - 30$ measurements (5 points per specimen, $1 - 6$ specimens per sample). This procedure makes up for the high within- and between-shell variability for Mg/Ca (Rathmann et al., 2004). Outliers beyond the 2σ range were discarded. The standard errors of the averages range from 0.1 to 0.4mmol/mol for Mg/Ca. The results of the $2 - 5$ samples per gravity core were combined to one LGM-data point.

Stable isotopes were measured after the trace element measurements on the same shells. The $\delta^{13}C$- and $\delta^{18}O$-values were determined on a Finnigan MAT 251 mass spectrometer equipped with an automated carbonate device. The analytical errors (1σ) are 0.07 for $\delta^{18}O$ and 0.03 for $\delta^{13}C$. The reproducibilities based on a laboratory standard are < 0.07 for $\delta^{18}O$ and < 0.05 for $\delta^{13}C$.

4.2.5. Reconstruction of bottom water temperature (BWT) and density

The Mg/Ca ratios and $\delta^{18}O_c$ values were used to reconstruct bottom water temperatures (BWT) and water mass densities (ρ). We used the BWT–Mg/Ca relationship from Rathmann et al. (2004) for the reconstruction of the BWT ($\mathrm{Mg/Ca} = 1.528 * e^{(0.09*\mathrm{BWT})}$, where Mg/Ca is reported in mmol/mol and BWT is the bottom water temperature in °C). These BWT were used to subtract the temperature component from foraminiferal $\delta^{18}O$ in order to calculate $\delta^{18}O_{sw}$ and paleosalinity following the procedure in Wolff et al. (1999, equations 2 and 7): $\delta^{18}O_w = \delta^{18}O_c - 21.9 + \sqrt{310.6 + 10 * BWT}$ and $\mathrm{S} = \dfrac{\delta^{18}O_w - b}{a} - \dfrac{d_g}{a} + S_g$ with the isotope ratio of seawater $\delta^{18}O_w$, the isotope ratio of the foraminifera test $\delta^{18}O_c$ and the above calculated

Table 4.2.: Reconstructed BWT and density.

(a) Multicorer

core number	Depth, m	Lat., °S	Lon., °E	$\delta^{18}O_c$, ‰ VPDB	$\delta^{18}O_w$, ‰ VPDB	S, psu	ρ, kg/m^3
GeoB 8403-1	320	24.25	13.61	1.72	0.49	35.32	1028.57
GeoB 8452-1	388	25.46	13.68	2.11	0.40	35.14	1029.08
GeoB 8450-1	506	25.47	13.61	2.30	-0.22	34.00	1029.02
GeoB 8449-1	605	25.48	13.55	2.30	0.004	34.41	1029.93
GeoB 3717-1	855	24.83	13.35	2.74	-0.18	34.08	1031.01
GeoB 8430-2	1330	25.61	13.28	3.01	-0.31	33.83	1033.06

(b) Gravity corer

GeoB 8452-2	387	25.46	13.68	1.89	1.25	35.59	1028.04
GeoB 8453-1	505	25.47	13.61	2.78	1.32	35.72	1029.32
GeoB 8448-1	803	25.48	13.45	3.51	1.79	36.60	1031.52
GeoB 8426-2	1045	25.48	13.35	4.12	1.84	36.70	1033.05
GeoB 8455-3	1515	25.51	13.18	4.52	1.69	36.42	1035.26
GeoB 3606-1	1785	25.47	13.08	5.10	0.81	34.79	1035.82

bottom water temperature BWT. a is the slope of the $\delta^{18}O_w$–salinity relationship and b is the freshwater end member of $\delta^{18}O$. d_g and S_g are correction factors for $\delta^{18}O_w$ and salinity. They are 0 for the core tops and 1.2‰ and 1.1‰, respectively, for the gravity core samples. These reconstructed BWT and paleosalinities were used to calculate ρ with an online calculator (Tomczak, 2000). See all data in Table 4.2.

Table 4.3.: Time slice measurements (LGM) of the cores.

GC number	Depth, m	Lat., °S	Lon., °E	Mg/Ca, $\frac{\text{mmol}}{\text{mol}}$	deviation	$\delta^{18}O_c$, ‰ VPDB
GeoB 8452-2	387	25.46	13.68	4.921	0.75	1.886
GeoB 8453-1	505	25.47	13.61	3.630	0.67	2.780
GeoB 8448-1	803	25.48	13.45	3.311	0.12	3.506
GeoB 8426-2	1045	25.48	13.35	2.715	0.38	4.122
GeoB 8455-3	1515	25.51	13.18	2.251	0.11	4.517
GeoB 3606-1	1785	25.47	13.08	1.398	0.09	5.102

4.3. Results

The temperature drops from ~ 11°C in shallowest down to ~ 3°C at the deepest sites.

The Mg/Ca ratios generally decrease with increasing water depth, ranging from $\sim$ 4mmol/mol to $\sim$ 2mmol/mol at the sediment surface and from 4.9mmol/mol to 1.4mmol/mol for the LGM samples (see Table 4.3 and Figure 4.3). The Mg/Ca ratios for the LGM are slightly higher than the Holocene values (~ 0.8mmol/mol on average), except for the deepest gravity core GeoB 3606-1 (Figure 4.3). In the same depth interval, $\delta^{18}O_c$ increase from 1.886‰ to 5.102‰. When the LGM data are corrected for sea level (1‰) there are nearly no differences between the gravity core data and the multicorer data (see the equlibrium curve in Figure 4.3).

The calculated modern seawater salinity fluctuates between 35.32psu at the shallowest depth and 33.83psu (Table 4.2a) at the deepest core position and is $< 1\%$ lower than the measured data (Moorholz and Heene, 2003a). For the LGM the seawater salinity is slightly higher, as expected, we have a scope from 34.79psu to 36.7psu (Table 4.2b).

The seawater density was calculated to verify, that the water masses follow the correct sequence. Each water mass has a different density, increasing with increasing water depth. The calculated in-situ density span the range from $1028.57 kgm^{-3}$ for the shallowest multicore to $1033.06 kgm^{-3}$ for the deepest multicore. For the multicores from M57/2, CTD-data for the density is available. These measured density data (Moorholz and Heene, 2003a) are slightly lower ($< 0.5\%$) than the calculated ones, but the offset is not constant. Due to the absence of CTD-data for all multicores and the variable differences, the offset will be ignored. For the gravity cores the range is $1028.04 - 1035.82 kgm^{-3}$. Figure 4.4 show the calculated seawater densities against water depth. Both multicorer (Figure 4.4, black dots) and gravity corer data (Figure 4.4, red dots) show these increases of water depth and sewater density.

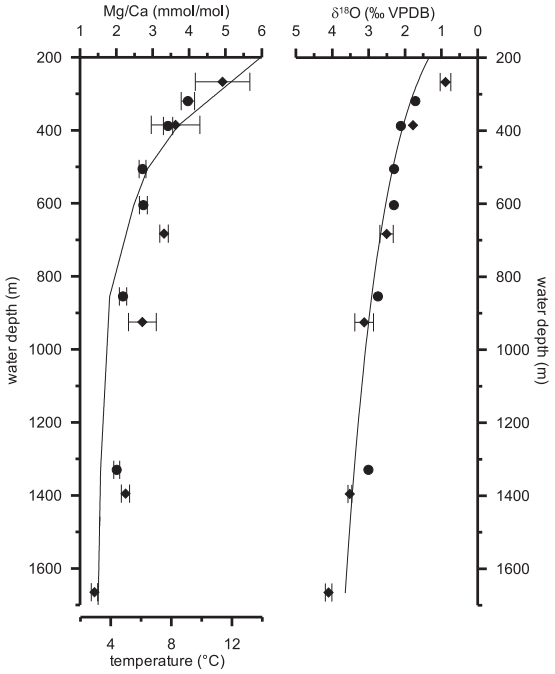

Figure 4.3.: Mg/Ca and $\delta^{18}O$ measurement data. Dots denote multicorer data (modern), diamonds denote gravity core data (LGM, corrected for sealevel change, $\delta^{18}O$ is correted for the ice effect of 1‰). Left curve specifies the BWT nowadays. Right curve is the equilibrium water line ($\delta^{18}O_{eq}$).

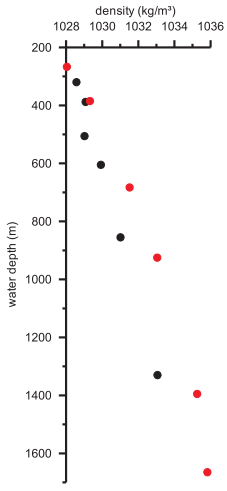

Figure 4.4.: Sea water density ρ against water depth. Black dots denote multicorer data, red dots denote gravity core data.

4.4. Discussion and Conclusions

Our data show that both glacial $\delta^{18}O$ and Mg/Ca values in the upper 400m of the water column off Namibia were not significantly different from modern ones. However, at intermediate depths, below about 600m, we find a small but significant warming of $1-2$°C together with slightly higher $\delta^{18}O$ values. This indicates a slightly lower thermal stratification together with a somewhat higher salinity stratification of upper water masses in this region. Calculation of seawater density indicates that both the modern and the glacial distributions of Mg/Ca and $\delta^{18}O$ resulted in a stable stratification of the water column when translated into temperature and salinity. Our data are also consistent with the $\delta^{18}O$ compilation of Lynch-Stieglitz et al. (2006), which shows a reversal of the modern zonal density gradient across the South Atlantic during the LGM, which can be interpreted as an upward movement of isotherms in the west and a downward movement of isotherms in the east with respect to the present-day situation. In summary, we cannot reject a glacial circulation pattern with a more vigorous northward flow of Antarctic Intermediate Water balanced by a southward flow of surface waters as suggested by Lynch-Stieglitz et al. (2006). However, the assessment whether the east west density gradient was indeed reversed during the LGM, would require Mg/Ca measurements on vertical core profiles in the western Atlantic which are currently not available.

Our reconstruction of the water column structure also has implications for the source of the glacial cooling in the eastern upwelling system off Namibia. It has been speculated that at least a fraction of the LGM cooling of up to $8-10$°C observed in the upwelling system off Namibia was due to a change in the preformed temperature of the source waters of the upwelling. Modeling experiments have shown that a doubling of the wind stress would lead to a $2-3$°C cooling in the upwelling area off Namibia (Paul and Schäfer-Neth, 2003). This would leave $5-6$°C to be explained by other mechanisms. Our study indicates that changes in the temperature of the South Atlantic Central Water were small and cannot be a strong contributor of the glacial surface cooling off Namibia. Rather strong regional coolings might be explained by an offshore movement of upwelling cells during the glacial lowstands. Today most of the upwelling takes place on the shelf and at the shelf edge where no glacial deposits can be found. Within the upwelling temperature can be more than 5°C lower than in the adjacent open ocean (Stephens et al., 2002). During sea level lowering the upwelling cells moved from the shelf to the upper continental slope. Thus many of the core locations used for SST reconstructions experienced a regime shift from direct upwelling during glacial lowstands to open ocean conditions today. Hence the strong cooling seems to be caused by a frontal shift rather than a change in preformed temperatures of source waters.

Acknowledgements This work was funded by the Deutsche Forschungsgemeinschaft (DFG Research Center Ocean Margins Contribution No. RCOMxxxx).

5. Conclusions and Outlook

This study demonstrates clearly that measuring Mg/Ca ratios on *O. umbonatus* with the laser ablation technique is a useful alternative approach to estimate bottom water temperatures. Since *O. umbonatus* is abundant over the main thermocline, it is a good candidate for studying past variations in vertical temperature gradients. The investigation of surface samples to calibrate this proxy for the Benguela Upwelling Area revealed the following results:

- The sensitivity of the Mg/Ca–temperature relationship for *O. umbonatus* is comparable to that of *Cibicidoides* spp.
- The laser ablation technique allows the rapid determination of Mg/Ca ratios as long as the number of samples is relatively small. It is therefore well suited for overviews on core sequences and can serve as a basis for subsequent high-resolution studies with liquid solution analyses.
- Laser ablation also provides information on within-sample variability that is otherwise difficult to obtain.
- The high number of measurements per sediment sample allows identification of outliers and potentially contaminated shell parts and their subsequent exclusion, thus increasing the accuracy of the final temperature estimate.

Research findings of the last years have shown, that the carbonate ion concentration / saturation can have an influence on the incorporation of trace elements and stable isotopes in the tests of foraminifera. Therefore it was necessary to examine, whether such an influence could also be detected for *O. umbonatus*. This study showed:

- There is a negative correlation between $\delta^{18}O_{corr}$ and [CO_3^{2-}], which has been expected from previous observations and experiments. However, the variability in $\delta^{18}O_{corr}$ between the various sample stations is small, and we suggest further investigation covering a broader range of values.
- A significant [CO_3^{2-}] dependence was inferred for Sr/Ca, which accounts for most of the Sr/Ca variability. In contrast to previous studies, the sign of the relationship is negative, yet the results indicate that Sr/Ca in *O. umbonatus* has the potential to be used as a paleo-proxy for pore-water [CO_3^{2-}].
- The influence of [CO_3^{2-}] on the trace element ratios and stable isotope composition appears to be more important than the influence of $\Delta[CO_3^{2-}]$.
- No clear influence of [CO_3^{2-}] was observed for $\delta^{13}C$ and Mg/Ca.

- Depending on the habitat of the investigated foraminiferal species it is important to distinguish between the chemical properties of the pore-water and the water column. For organic-rich sediments it is necessary to use pore-water measurements to investigate the influence of the carbonate system on the shell composition of endobenthic foraminifera like *O. umbonatus*.

Niebler et al. (2003) have speculated that at least a fraction of the LGM cooling of up to $8-10$°C observed in the upwelling system off Namibia was due to a change in the preformed temperature of the source waters of the upwelling. Modeling experiments have shown that a doubling of the wind stress would lead to a $2-3$°C cooling in the upwelling area off Namibia (Paul and Schäfer-Neth, 2003). This would leave $6-7$°C to be explained by other mechanisms. Investigating trace elements and stable isotopes of *O. umbonatus* in the LGM time slice of the sedimentary record within the Benguela Upwelling Area has shown:

- Both glacial $\delta^{18}O$ and Mg/Ca values in the upper 400m of the water column off Namibia were not significantly different from modern ones. At intermediate depths, below about 600m, a small but significant warming of $1-2$°C together with slightly higher $\delta^{18}O$ values was found. This indicates a slightly lower thermal stratification together with a somewhat higher salinity stratification of upper water masses in this region.

- The calculation of seawater density indicates that both the modern and the glacial distributions of Mg/Ca and $\delta^{18}O$ resulted in a stable stratification of the water column when translated into temperature and salinity.

- Changes in the temperature of the South Atlantic Central Water were small and cannot be a strong contributor to the glacial surface cooling off Namibia. Rather strong regional coolings might be explained by an offshore movement of upwelling cells during the glacial lowstands. During sea level lowering in the LGM the upwelling cells moved from the shelf to the upper continental slope. Thus many of the core locations used for SST reconstructions experienced a regime shift from direct upwelling during glacial lowstands to open ocean conditions today. Hence the strong cooling seems to be caused by a frontal shift rather than a change in preformed temperatures of source waters.

This work shows a regional investigation on the rarely used species *O. umbonatus*. For future studies, it would be interesting to do the same analysis in other regions of the Atlantic Ocean, e.g. off NW-Africa as well as in upwelling areas in the other oceans. The area off NW-Africa between Cape Blanc in the south ($\sim$ 22°N) and Cape Ghir in the north ($\sim$ 30°N) seems a good candidate for further investigations of that kind, due to the numerous expeditions conducted in the recent past (Meggers and cruise participants, 2002; Schulz and cruise participants, 2003; Bleil and cruise participants, 2004). The oceanographic situation is as well known as off Namibia, and the sample frequency of GeoB sediment cores is nearly the same. In addition, the geochemistry group at Bremen University also does extensive investigations in the region, so that the geochemical parameters like $[CO_3^{2-}]$ are available for the water column as well as for the pore-water. A comparison of the different calibrations for

the Mg/Ca–BWT-relationship might lead to a more general calibration and give more information about the $\delta^{18}O$–[CO_3^{2-}]-interaction.

Another interesting topic for future research is the investigation of other species in the same region, e.g. *C. wuellerstorfi* in the deeper part of the shelf. Based on the conclusion of this work, that regional calibrations for benthic foraminifera are more accurate, it would be interesting to see, if there are also differences between the regions. *C. wuellerstorfi* is a common benthic species for paleoceanographic reconstructions. Its Mg/Ca–temperature calibration is based on a global set of measurements. Regional investigations are rare (Raitzsch et al., 2008) and recent research is often still on a global scale (Healey et al., 2008), but a regional calibration was never investigated in detail.

A. Additional material

A.1. Additional Figure to Chapter 3, Mg/Ca- and Sr/Ca-measurements

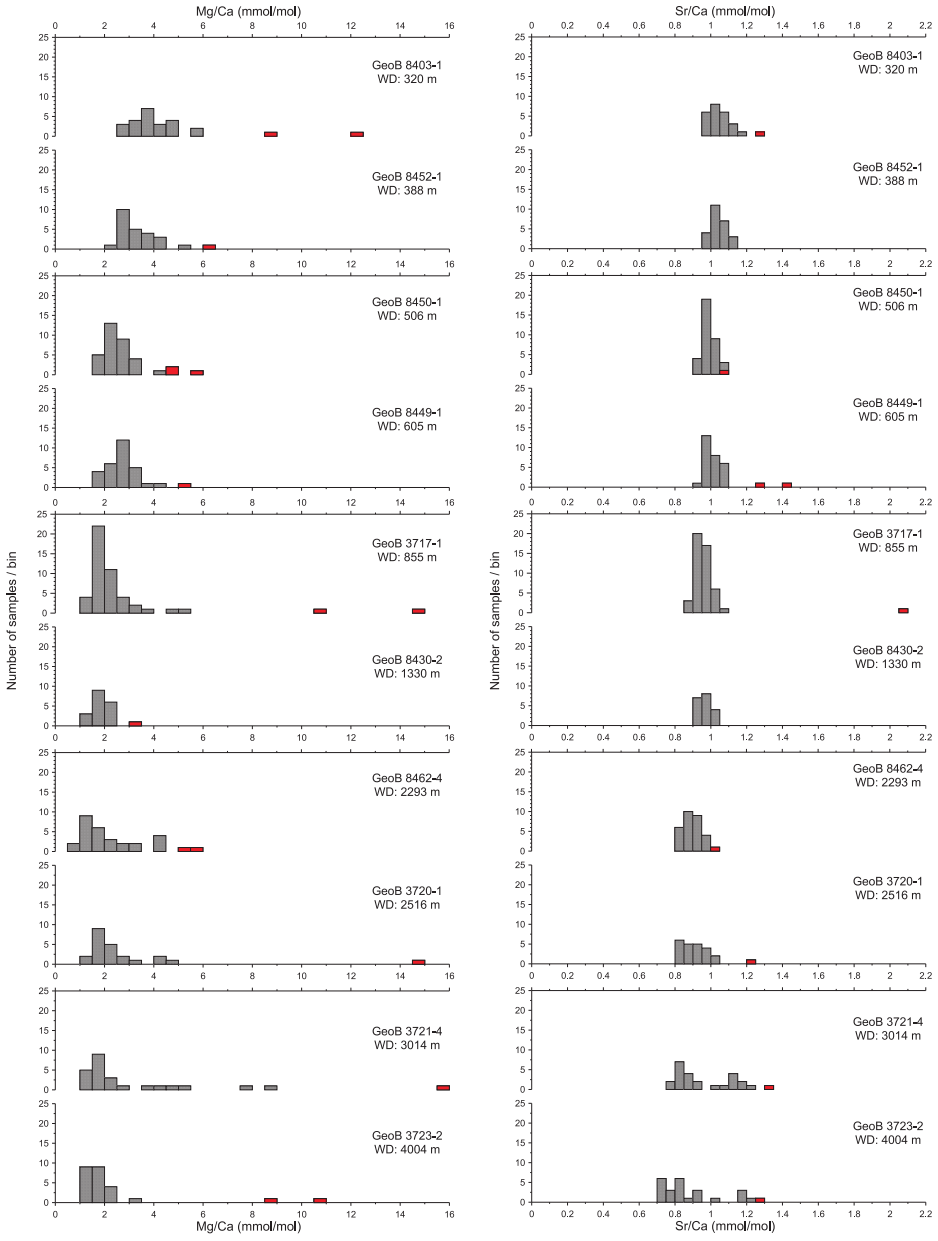

Figure A.1.: Histogram of single Mg/Ca and Sr/Ca measurements. Red bars denote outliers.

A.2. Additional Material to Chapter 3, stable isotope measurements

To investigate the potential impact of laser ablation on the stable isotopic composition (for example, due to fractionation in the vapour and subsequent condensation on the sample), we additionally measured fresh (not ablated) sample splits for M57/2. Each of these parallel splits consisted of five tests. Shells that have been subject to laser ablation tend to have marginally lighter isotopic values within the analytical uncertainty (Figure A.2). This suggests that laser ablation does not induce significant artefacts in the remaining shell material (for example, through preferential evaporation of isotopically lighter and condensation of isotopically heavier material). Our approach of analyzing the elemental and isotopic compositions on the same foraminiferal tests is therefore valid.

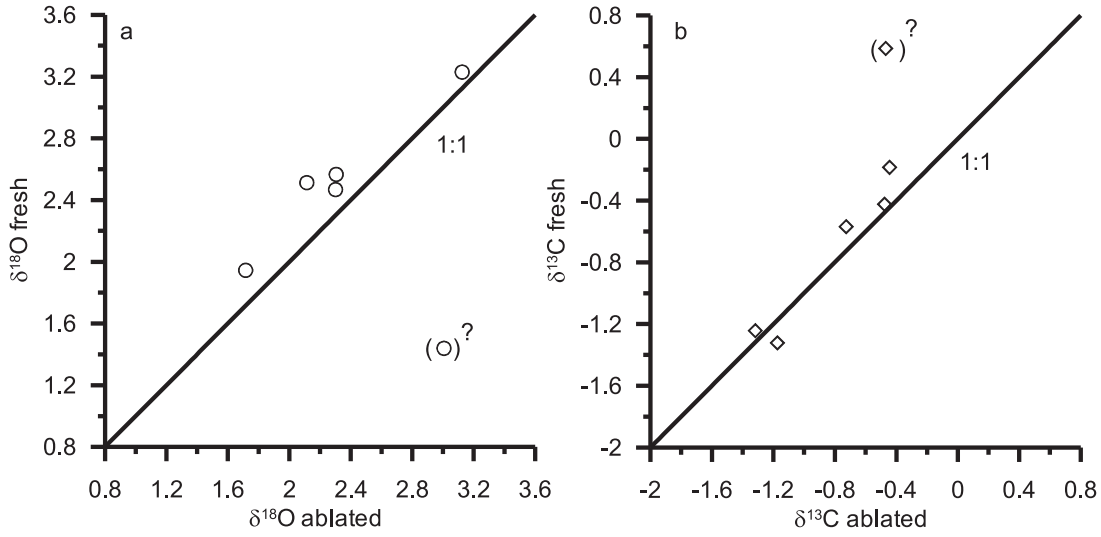

Figure A.2.: Comparison of stable isotope measurements of previously ablated test and fresh tests.

B. References

Alibert, C. and M. T. McCulloch (1997). Strontium/calcium ratios in modern *Porites* corals from the Great Barrier Reef as a proxy for sea surface temperature: Calibration of the thermometer and monitoring of ENSO. *Paleoceanography 12*(3), 345–364.

Anand, P. and H. Elderfield (2005). Variability of Mg/Ca and Sr/Ca between and within the planktonic foraminifers *Globigerina bulloides* and *Globorotalia truncatulinoides*. *Geochem. Geophys. Geosys. 6*(11), Q11D11, doi: 10.1029/2004GC000811.

Anand, P., H. Elderfield, and M. Conte (2003). Calibration of Mg/Ca thermometry in planktonic foraminifera from a sediment trap time series. *Paleoceanography 18*, doi:10.1029/2002PA000846.

Arai, T., T. Hirata, and Y. Takagi (2006). Application of laser ablation ICPMS to trace the environmental history of chum salmon *Oncorhynchus keta*. *Mar. Env. Res. 63*, 55–66.

Archer, D., S. Emerson, and C. E. Reimers (1989). Dissolution of calcite in deep-sea sediments: pH and O_2 microelectrode results. *Geochim. Cosmochim. Acta 53*, 2831–2845.

Barker, S., I. Cacho, H. Benway, and K. Tachikawa (2005). Planktonic foraminiferal Mg/Ca as a proxy for past oceanic temperatures: a mehodological overview and data compilation for the Last Glacial Maximum. *Quat. Sci. Rev. 24*, 821–834.

Barker, S., M. Greaves, and H. Elderfield (2003). A study of cleaning procedures used for foraminiferal Mg/Ca paleothermometry. *Geochem. Geophys. Geosys. 4*(9), 8407, doi:10.1029/2003GC000559.

Bauch, D., H. Erlenkeuser, G. Winckler, G. Pavlova, and J. Thiede (2002). Carbon isotopes and habitat of polar planktic foraminifera in the Okhotsk Sea: The 'carbonate ion effect' under natural conditions. *Mar. Micropal. 45*, 83–99.

Beck, J. W., R. L. Edwards, E. Ito, F. W. Taylor, J. Recy, F. Rougerie, P. Joannot, and C. Henin (1992). Sea-surface temperature from coral skeletal strontium/calcium ratios. *Science 257*, 644–647.

Bernstein, R. E., P. R. Betzer, R. A. Feely, R. H. Byrne, M. Lamb, and A. F. Michaels (1987). Acantharian Fluxes and Strontium to Chlorinity Ratios in the North Pacific Ocean. *Science 237*, 1490–1494.

Billups, K. and D. P. Schrag (2003). Application of benthic foraminiferal Mg/Ca ratios to questions of Cenozoic climate change. *Earth Planet. Sci. Lett. 209*, 181–195.

Bleil, U. and cruise participants (1996). *Report and preliminary results of METEOR Cruise M34/1, Cape Town – Walvis Bay, 03.01.1996 – 26.01.1996*. Number 77 in Berichte aus dem Fachbereich Geowissenschaften. Fachbereich Geowissenschaften, Universität Bremen.

Bleil, U. and cruise participants (2004). *Report and preliminary results of METEOR Cruise M58/2, Las Palmas – Las Palmas (Canary Islands, Spain), 15.05. – 08.06.2003*. Number 227 in Berichte aus dem Fachbereich Geowissenschaften. Fachbereich Geowissenschaften, Universität Bremen.

Boyle, E. and J. Erez (2003). Does carbonate ion influence foraminiferal Mg/Ca? *Ocean Sci. Meet. Suppl. AGU 84*, Abstract OS21G–01.

Boyle, E. A. and L. D. Keigwin (1985). Comparison of Atlantic and Pacific paleochemical records for the last 250,000 years: Changes in deep ocean circulation and chemical inventories. *Earth Planet. Sci. Lett. 76*, 135–150.

Broecker, W. S. and T.-H. Peng (1982). *Tracers in the Sea*. Lamont-Doherty Geological Observatory, Columbia University, Palisades, New York.

Brown, S. J. and H. Elderfield (1996). Variations in Mg/Ca and Sr/Ca ratios of planktonic foraminifera caused by postdepositional dissolution: Evidence of shallow Mg-dependent dissolution. *Paleoceanography 11*, 543–551.

CLIMAP-Project Members (1981). Seasonal Reconstruction of the Earth's Surface at the last Glacial Maximum. *Geol. Soc. Amer. Map Chart Ser. MC-36*, 1–18.

Conkright, M. E., R. A. Locarnini, H. E. Garcia, T. D. O'Brien, T. P. Boyer, C. Stephens, and J. I. Antonov (2002). *World OceanAtlas 2001: Objective Analyses, Data Statistics, and Figures, CD-ROM Documentation*. National Oceanographic Data Center, Silver Spring, MD.

Corliss, B. H. (1985). Microhabitats of benthic foraminifera within deep-sea sediments. *Nature 314*, 435–438.

Corliss, B. H. (1991). Morphology and microhabitat preferences of benthic foraminifera from the northwest Atlantic Ocean. *Mar. Micropal. 17*, 195–236.

De Deckker, P., A. R. Chivas, and J. M. G. Shelley (1999). Uptake of Mg and Sr in the euryhaline ostracod *Cyprideis* determined from in vitro experiments. *Palaeogeogr., Palaeoclim., Palaeoecol. 148*, 105–116.

de Villiers, S. (1999). Seawater strontium and Sr/Ca variability in the Atlantic and Pacific oceans. *Earth Planet. Sci. Lett. 171*, 623–634.

Dekens, P. S., D. W. Lea, D. K. Pak, and H. J. Spero (2002). Core top calibration of Mg/Ca in tropical foraminifera: Refining paleotemperature estimation. *Geochem. Geophys. Geosys. 3*(4), 10.1029/2001GC000200.

Dickson, A. G. (1990). Standard potential of the reaction: AgCl(s) + 1/2 H_2(g) = Ag('s') + HCl(aq), and the standard acidity constant of the ion HSO_4^- in synthetic seawater from 273.15 to 318.15 K. *J. Chem. Thermodyn. 22*, 113–127.

Eggins, S., P. De Deckker, and J. Marshall (2003). Mg/Ca variation in planktonic foraminifera tests: implications for reconstructing paleo-seawater temperature and habitat migration. *Earth Planet. Sci. Lett. 212*, 291–306.

Eggins, S. M., A. Sadekov, and P. De Deckker (2004). Modulation and daily banding of Mg/Ca in *Orbulina universa* tests by symbiont photosynthesis and respiration: a complication for seawater thermometry? *Earth Planet. Sci. Lett. 225*, 411–419.

Elderfield, H. and G. Ganssen (2000). Past temperature and δ^{18}O of surface ocean waters inferred from foraminiferal Mg/Ca ratios. *Nature 405*, 442–445.

Elderfield, H., J. Yu, P. Anand, T. Kiefer, and B. Nyland (2006). Calibrations for benthic foraminiferal Mg/Ca paleothermometry and the carbonate ion hypothesis. *Earth Plant. Sci. Lett. 250*(3-4), 633–649.

Emiliani, C. (1955). Pleistocene temperatures. *J. Geol. 63*, 538–578.

Epplé, V. M. (2004). *High-resolution climate reconstruction for the Holocene based on growth chronologies of the bivalve Arctica islandica from the North Sea*. Ph. D. thesis, University Bremen.

Epstein, S., R. Buchsbaum, H. A. Lowenstam, and U. H. C. (1953). Revised carbonate-water isotopic temperature scale. *Bull. Geol. Soc. Amer. 64*, 1315–1325.

Fairbanks, R. G. (1989). A 17,000-year glacio-eustatic sea level record: influence of glacial melting rates on the Younger Dryas event and deep-ocean circulation. *Nature 342*, 637–642.

Fallon, S. J., M. T. McCulloch, R. van Woesik, and D. J. Sinclair (1999). Corals at their latitudinal limits: laser ablation trace element systematics in *Porites* from Shirigai Bay, Japan. *Earth Planet. Sci. Lett. 172*(3-4), 221–238.

Fehrenbacher, J., P. A. Martin, and G. Eshel (2006). Glacial deep water carbonate chemistry inferred from foraminiferal Mg/Ca: A case study from the western tropical Atlantic. *Geochem. Geophys. Geosys. 7*(9), Q09P16, doi:10.1029/2005GC001156.

Felis, T., G. Lohmann, H. Kuhnert, S. J. Lorenz, D. Scholz, J. Pätzold, S. A. Al-Rousan, and S. M. Al-Moghrabi (2004). Increased seasonality in Middle East temperatures during the last interglacial period. *Nature 429*, 164–168.

Fennel, W. (1999). Theory of the Benguela upwelling system. *J. Phys. Oceanogr. 29*, 177–190.

Fischer, G., P. J. Müller, and G. Wefer (1998). Latitudinal $\delta^{13}C_{org}$ variations in sinking matter and sediments from the South Atlantic: Effects of anthropogenic CO_2 and implications for paleo-PCO_2 reconstructions. *J. Mar. Syst. 17*, 471–495.

Fischer, G. and G. Wefer (Eds.) (1999). *Use of Proxies in Paleoceanography: Examples from the South Atlantic*. Springer Verlag Berlin Heidelberg.

Giraudeau, J., G. W. Bailey, and C. Pujol (2000). A high-resolution time-series analyses of particle fluxes in the Northern Benguela coastal upwelling system: Carbonate record of changes in biogenic production and particle transfer processes. *Deep Sea Res., Part II 47*, 1999–2028.

Gooday, A. J. (1994). The biology of deep-sea foraminifera: a review of some advances and their applications in paleoceanography. *Palaios 9*, 14–31.

Hales, B. and S. Emerson (1996). Calcite dissolution in sediments of the Ontong-Java Plateau: In situ measurements of pore water O_2 and pH. *Global Biogeochem. Cycles 10*(3), 527–541.

Harriss, R. C. and C. C. Almy (1964). A preliminary investigation into the incorporation of minor elements into skeletal material of scleractinian corals. *Bull. Mar. Sci. Caribb. 14*, 418–423.

Hathorne, E. C., O. Alard, R. H. James, and N. W. Rogers (2003). Determination of intratest variability of trace elements in foraminifera by laser ablation inductively coupled plasma-mass spetrometry. *Geochem. Geophys. Geosys. 4*(12), 8408, doi:10.1029/2003GC000539.

Healey, S. L., R. C. Thunell, and B. H. Corliss (2008). The Mg/Ca-temperature relationship of benthic foraminiferal calcite: New core-top calibrations in the < 4°C temperature range. *Earth Planet. Sci. Lett. 272*, 523–530.

Hensen, C., H. Landenberger, M. Zabel, and H. D. Schulz (1998). Quantification of diffusive benthic fluxes of nitrate, phosphate, and silicate in the southern Atlantic Ocean. *Global Biogeochem. Cycles 12*(1), 193–210.

Hensen, C., M. Zabel, and H. D. Schulz (2000). A comparison of benthic nutrient fluxes from deep-sea sediments off Namibia and Argentina. *Deep-Sea Res. II 47*, 2029–2050.

Houghton, J. T., Y. Ding, D. J. Griggs, M. Noguer, P. J. van der Linden, and D. Xiaosu (2001). Climate Change 2001: The Scientific Basis. Technical report, Cambridge University Press.

Houghton, J. T., L. G. Meira Filho, B. A. Callander, N. Harris, A. Kattenberg, and K. Maskell (1995). Climate Change 1995 - The Science of Climate Change. Technical report, Cambridge University Press.

Johnson, G. C. and M. J. McPhaden (1999). Interior pycnocline flow from the Subtropical to the Equatorial Pacific Ocean. *J. Phys. Oceanogr. 29*(12), 3073–3089.

Karstensen, J. and D. Quadfasel (2002). Water subducted into the Indian Ocean subtropical gyre. *Deep-Sea Res. II 49*, 1441–1457.

Katz, A. (1973). The interaction of magnesium with calcite during crystal growth at $25 - 90°$C and one atmosphere. *Geochim. Cosmochim. Acta 37*, 1563–1578.

Katz, A., E. Sass, A. Starinsky, and H. D. Holland (1972). Strontium behavior in the aragonite-calcite transformation: An experimental study at 40-98°C. *Geochim. Cosmochim. Acta 36*, 481–496.

Key, R. M.and Kozyr, A., C. L. Sabine, K. Lee, R. Wanninkhof, J. L. Bullister, R. A. Feely, F. J. Millero, C. Mordy, and T.-H. Peng (2004). A global ocean carbon climatology: Results from GlobalData Analysis Project (GLODAP). *Global Biogeochem. Cycl. 18*, GB4031, doi:10.1029/2004GB002247.

Kinsman, D. J. J. (1969). Interpretation of Sr^{2+} concentrations in carbonate minerals and rocks. *J. Sedim. Petrol. 39*, 486–508.

Lea, D., D. Pak, and H. Spero (2000). Climate impact of late quaternary equatorial Pacific sea surface temperature variations. *Science 289*, 1719–1724.

Lea, D. W. (1999). Trace elements in foraminiferal calcite. In B. K. Sen Gupta (Ed.), *Modern Foraminifera*, pp. 259–277. Kluwer Academic Publishers.

Lea, D. W., T. A. Mashiotta, and H. J. Spero (1999). Controls on magnesium and strontium uptake in planktonic foraminifera determined by live culturing. *Geochim. Cosmochim. Acta 63*(16), 2369–2379.

Lear, C. H., H. Elderfield, and P. A. Wilson (2000). Cenocoic Deep-Sea Temperatures and Global Ice Volumes from Mg/Ca in Benthic Foraminiferal Calcite. *Science 287*, 269–272.

Lear, C. H., Y. Rosenthal, and N. Slowey (2002). Benthic foraminiferal Mg/Ca-paleothermometry: A revised core-top calibration. *Geochim. Cosmochim. Acta 66*(19), 3375–3387.

Levitus, S. and T. P. Boyer (1994). *World Ocean Atlas 1994, Vol. 4: Temperature. NOAA Atlas NESDIS 4*. U.S. Gov. Printing Office, Washington, D.C.

Lewis, E. and D. W. R. Wallace (1998). *Program developed for CO_2 system calculations, ORNL/CDIAC-105*. Carbon Dioxide Information Analysis Center, Oak Ridge National Laboratory, U.S. Department of Energy, Oak Ridge, Tennessee.

Lutjeharms, J. R. E. and J. M. Meeuwis (1987). The extent and variability of south-east Atlantic upwelling. *S. Afr. J. Mar. Sci. 5*, 51–62.

Lutjeharms, J. R. E. and P. L. Stockton (1987). Kinematics of the upwelling front off southern Africa. *S. Afr. J. Mar. Sci. 5*, 35–49.

Lutze, G. F. and H. Thiel (1989). Epibenthic foraminifera from elevated microhabitats: *Cibicidoides wuellerstorfi* and *Planulina arimiensis*. *J. Foraminiferal Res. 19*, 153–158.

Luyten, J. R., J. Pedlosky, and H. Stommel (1983). The ventilated thermocline. *J. Phys. Oceanogr. 13*(2), 292–309.

Lynch-Stieglitz, J., W. B. Curry, D. W. Oppo, U. S. Ninneman, C. D. Charles, and J. Munson (2006). Meridional overturning circulation in the South Atlantic at the last glacial maximum. *Geochem. Geophys, Geosys. 7*, Q10N03, doi:10.1029/2005GC001226.

Mackensen, A. and T. Bickert (1999). Stable Carbon Isotopes in Benthic Foraminifera: Proxies for Deep and Bottom Water Circulation and New Production. In G. Fischer and G. Wefer (Eds.), *Use of Proxies in Paleoceanography: Examples from the South Atlantic*, pp. 229–254. Springer Verlag Berlin Heidelberg.

Malone, M. J. and P. A. Baker (1999). Temperature dependence of the strontium distribution coefficient in calcite: An experimental study from 40^0 to 200^0C and application to natural diagenetic calcites. *J. Sed. Res. 69*(1), 216–223.

Martin, P. A. and D. W. Lea (2002). A simple evaluation of cleaning procedures on fossil benthic foraminiferal Mg/Ca. *Geochem. Geophys. Geosys. 3*(10), 8401, doi:10.1029/2001GC000280.

Martin, P. A., D. W. Lea, T. A. Mashiotta, T. Papenfuss, and M. Sarnthein (1999). Variation on foraminiferal Sr/Ca over Quaternary glacial-interglacial cycles: Evidence for changes in mean ocean Sr/Ca? *Geochem. Geophys. Geosys. 1*(1), doi:10.1029/1999GC000006.

Martin, P. A., D. W. Lea, Y. Rosenthal, N. J. Shackleton, M. Sarnthein, and T. Papenfuss (2002). Quaternary deep sea temperature histories derived from benthic foraminiferal Mg/Ca. *Earth Planet. Sci. Lett. 198*, 193–209.

McCorkle, D. C., L. D. Keigwin, B. H. Corliss, and S. R. Emerson (1990). The influence of microhabitats on the carbon isotopic composition of deep-sea benthic foraminifera. *Paleoceanography 5*(2), 161–185.

McCorkle, D. C., P. A. Martin, D. W. Lea, and G. P. Klinkhammer (1995). Evidence of a dissolution effect on benthic foraminiferal shell chemistry: δ^{13}C, Cd/Ca, Ba/Ca, and Sr/Ca results from the Ontong Java Plateau. *Paleoceanography 10*(4), 699–714.

McCrea, J. M. (1950). On the isotopic chemistry of carbonates and a paleotemperature scale. *J. Chem. Phys. 18*, 849–857.

Meggers, H. and cruise participants (2002). *Report of RV POSEIDON Cruise POS272, Las Palmas – Las Palmas, 1.4. – 14.4.2001*. Number 197 in Berichte aus dem Fachbereich Geowissenschaften. Fachbereich Geowissenschaften, Universität Bremen.

Müller, A. (2000). *Mg/Ca und Sr/Ca-Verhältnisse in biogenem Carbonat planktischer Foraminiferen und benthischer Ostracoden*, Volume 313 of *Berichte aus dem Institut für Meereskunde*. Institut für Meereskunde, Kiel.

Mollenhauer, G., M. Kienast, F. Lamy, H. Meggers, R. R. Schneider, J. M. Hays, and T. I. Eglinton (2005). An evaluation of ^{14}C age relationships between co-occuring foraminifera, alkenones, and total organic carbon in continental margin sediments. *Paleoceanography 20*, PA1016, doi:10.1029/2004PA001103.

Moorholz, V. and T. Heene (2003a). CTD-Probe and Water Sampling. In M. Zabel (Ed.), *Report and prelimiary results of METEOR Cruise M 57/2, Walvis Bay - Walvis Bay, 11.02.-12.03.2003*, pp. 34–35. Fachbereich Geowissenschaften, Universität Bremen.

Moorholz, V. and T. Heene (2003b). Hydrographic studies. In M. Zabel (Ed.), *Report and prelimiary results of METEOR Cruise M 57/2, Walvis Bay - Walvis Bay, 11.02.-12.03.2003*, pp. 129–133. Fachbereich Geowissenschaften, Universität Bremen.

Morishita, T., A. Tsurumi, and T. Kamiya (2007). Magnesium and strontium distributions within valves of a recent marine ostracode, *Neonesidea oligodentata*: Implications for paleoenvironmental reconstructions. *Geochem. Geophys. Geosys. 8*(7), Q07009, doi:10.1029/2007GC001585.

Mortyn, P., H. Elderfield, P. Anand, and M. Greaves (2005). An evaluation of controls on planktonic foraminiferal Sr/Ca: Comparison of water column and core-top data from a North Atlantic transect. *Geochem. Geophys. Geosyst. 6*(12), Q12007, doi:10.1029/2005GC001047.

Mulitza, S., H. Arz, S. K. von Mücke, C. Moos, H.-S. Niebler, J. Pätzold, and M. Segl (1999). The South Atlantic Carbon Isotope Record of Planktic Foraminifera. In G. Fischer and G. Wefer (Eds.), *Use of Proxies in Paleoceanography: Examples from the South Atlantic*, pp. 427–445. Springer Verlag Berlin Heidelberg.

Mulitza, S. and A. Paul (2003). Water sampling for Stable Isotopes and Nutrient Analysis. In M. Zabel (Ed.), *Report and preliminary results of METEOR Cruise M 57/2, Walvis Bay – Walvis Bay, 11.02.–12.02.2003*, pp. 35–37. Fachbereich Geowissenschaften, Universität Bremen.

Niebler, H.-S., H. W. Arz, B. Donner, S. Mulitza, J. Pätzold, and G. Wefer (2003). Sea surface temperatures in the equatorial and South Atlantic Ocean during the Last Glacial Maximum (23–19 ka). *Paleoceanography 18*(3), 1069, doi:10.1029/2003PA000902.

Nürnberg, D., J. Bijma, and C. Hemleben (1996). Assessing the reliability of magnesium in foraminiferal calcite as a proxy for water mass temperatures. *Geochim. Cosmochim. Acta 60*, 803–814.

Okai, T., A. Suzuki, H. Kawahata, S. Terashima, and N. Imai (2002). Preparation of a new Geological Survey of Japan geochemical reference material: Coral JCp-1. *Geostand. Newsletter 25*, 95–99.

Oomori, T., H. Kaneshima, Y. Maezato, and Y. Kitano (1987). Distribution coefficient of Mg^{2+} ions between calcite and solution at $10 - 50°C$. *Mar. Chem. 20*, 327–336.

Paul, A., S. Mulitza, J. Pätzold, and T. Wolff (1999). Simulation of Oxygen Isotopes in a Global Ocean Model. In G. Fischer and G. Wefer (Eds.), *Use of Proxies in Paleoceanography: Examples from the South Atlantic*, pp. 655–686. Springer Verlag Berlin Heidelberg.

Paul, A. and C. Schäfer-Neth (2003). Modeling the water masses of the Atlantic Ocean at the Last Glacial Maximum. *Paleoceanography 18*(3), 1058, doi:10.1029/2002PA000783.

Pearce, N. J. G., W. T. Perkins, J. A. Westgate, M. P. Gorton, S. E. Jackson, C. L. Neal, and S. P. Chenery (1997). A compilation of new and published major and trace element data for NIST SRM 610 and NIST SRM 612 glass reference materials. *Geostand. Newsletter 21*, 115–144.

Pfeifer, K., C. Hensen, M. Adler, F. Wenzhöfer, B. Weber, and H. D. Schulz (2002). Modeling of subsurface calcite dissolution, including the respiration and reoxidation processes of marine sediments in the region of equatorial upwelling off Gabon. *Geochim. Cosmochim. Acta 66*(24), 4247–4259.

Raitzsch, M., H. Kuhnert, J. Groeneveld, and T. Bickert (2008). Benthic foraminifer Mg/Ca anomalies in South Atlantic core top sediments and their implications for paleothermometry. *Geochem. Geophys. Geosys. 9*, Q05010, doi:10.1029/2007GC001788.

Rathburn, A. E. and B. H. Corliss (1994). The ecology of living (stained) deep-sea benthic foraminifera from the Sulu Sea. *Paleoceanography 9*, 87–150.

Rathburn, A. E. and P. De Deckker (1997). Magnesium and strontium composition of Recent benthic foraminifera from the Coral Sea, Australia and Prydz Bay, Antartica. *Mar. Micropal. 32*, 231–248.

Rathmann, S., S. Hess, H. Kuhnert, and S. Mulitza (2004). Mg/Ca ratios of the benthic foraminifera *Oridorsalis umbonatus* obtained by laser ablation from core top sediments: Relationship to bottom water temperature. *Geochem. Geophys. Geosyst. 5*(12), Q12013, doi:10.1029/2004GC000808.

Rathmann, S. and H. Kuhnert (2008). Carbonate ion effect on Mg/Ca, Sr/Ca and stable isotopes on the benthic foraminifera *Oridorsalis umbonatus* off Namibia. *Mar. Micropal. 66*, 120–133.

Reichart, G.-J., F. Jorissen, P. Anschutz, and P. R. D. Mason (2003). Single foraminifera test chemistry records the marine environment. *Geology 31*(4), 355–358.

Romanek, C. S., E. L. Grossmann, and J. W. Morse (1992). Carbon isotopic fractionation in synthetic aragonite and calcite: effects of temperature and precipitation rate. *Geochim. Cosmochim. Acta 56*, 419–430.

Romero, O., G. Mollenhauer, R. R. Schneider, and G. Wefer (2003). Oscillation of the siliceous imprint in the central Benguela Upwelling System from MIS 3 through to the early Holocene: the influence of the Southern Ocean. *J. Quat. Sci. 18*(8), 733–743.

Rosenthal, Y., E. A. Boyle, and N. Slowey (1997). Temperature control on the incorporation of magnesium, strontium, fluorine and cadmium into benthic foraminiferal

shells from Little Bahama Bank: Prospects for thermocline paleoceanography. *Geochim. Cosmochim. Acta 61*(17), 3633–3643.

Rosenthal, Y., C. H. Lear, D. W. Oppo, and B. K. Linsley (2006). Temperature and carbonate ion effect on Mg/Ca and Sr/Ca ratios in benthic foraminifera: Aragonitic species *Hoeglundina elegans*. *Paleoceanography 21*, PA1007, doi:10.1029/2005PA001158.

Rosenthal, Y., S. Peeron-Cashman, C. H. Lear, E. Bard, S. Barker, K. Billups, M. Bryan, M. L. Delaney, P. B. deMenocal, G. S. Dwyer, H. Elderfield, C. R. German, M. Greaves, D. W. Lea, T. M. M. Jr., D. K. Pak, G. L. Paradis, A. D. Russel, R. R. Schneider, K. Scheiderich, L. Stott, K. Tachikawa, E. Tappa, R. Thunell, M. Wara, S. Weldeab, and P. A. Wilson (2004). Interlaboratory comparison study of Mg/Ca and Sr/Ca measurements in planktonic foraminifera for paleoceanographic research. *Geochem. Geophys. Geosys. 5*(4), Q04D09, doi:10.1029/203GC000650.

Roy, R. N., L. N. Roy, K. M. Vogel, C. Porter-Moore, T. Pearson, C. E. Good, F. J. Millero, and D. M. Campbell (1993). The dissociation constants of carbonic acid in seawater at salinities 5 to 45 and temperatures 0 to 45^0C. *Mar. Chem. 44*, 249–267.

Roy, R. N., L. N. Roy, K. M. Vogel, C. Porter-Moore, T. Pearson, C. E. Good, F. J. Millero, and D. M. Campbell (1994). Erratum. *Mar. Chem. 45*, 337.

Roy, R. N., L. N. Roy, K. M. Vogel, C. Porter-Moore, T. Pearson, C. E. Good, F. J. Millero, and D. M. Campbell (1996). Erratum. *Mar. Chem. 52*, 183.

Russell, A., B. Hönisch, H. Spero, and D. Lea (2004). Effects of seawater carbonate ion concentration and temperature on shell U, Mg, and Sr in cultured planktonic foraminifera. *Geochim. Cosmochim. Acta 68*, 4347–4361.

Russell, A. D. and H. J. Spero (2000, February). Field examination of the oceanic carbonate ion effect on stable isotopes in planktonic foraminifera. *Paleoceanography 15*(1), 43–52.

Schäfer-Neth, C., A. Paul, and S. Mulitza (2005). Perspectives on mapping the MARGO reconstructions by variogram analysis/kriging and objective analysis. *Quat. Sci. Rev. 24*, 1083–1093.

Schmiedl, G. (1995). Late Quaternary benthic foraminiferal assemblages from the eastern South Atlantic Ocean: Reconstruction of deep water circulation and productivity changes. Technical report, Alfred Wegener Institute for Polar and Marine Research. pp. 207.

Schmiedl, G., A. Mackensen, and P. J. Müller (1997). Recent benthic foraminifera from the eastern South Atlantic Ocean: Dependence on food supply and water masses. *Mar. Micropal. 32*, 249–287.

Schulz, H. D. and cruise participants (1996). *Report and preliminary results of METEOR Cruise M34/2, Walvis Bay – Walvis Bay, 29.01.1996 – 18.02.1996*. Number 78 in Berichte aus dem Fachbereich Geowissenschaften. Fachbereich Geowissenschaften, Universität Bremen.

Schulz, H. D. and cruise participants (2003). *Report and preliminary results of METEOR Cruise M58/1, Dakar – Las Palmas, 15.04.2003 – 12.05.2003*. Number 215 in Berichte aus dem Fachbereich Geowissenschaften. Fachbereich Geowissenschaften, Universität Bremen.

Shackleton, N. (1974). Attainment of isotopic equilibrium between ocean water and the benthonic foraminifera genus *Uvigerina*: Isotopic changes in the ocean during the last glacial. *Colloq. Int. C. N. R. S. 219*, 203–209.

Shannon, L. V. (1985). The Benguela ecosystem, I, Evolution of the Benguela, physical features and processes. *Oceanogr. Mar. Biol. Ann. Rev. 23*, 105–182.

Shannon, L. V. and G. Nelson (1996). The Benguela: Large scale features and processes and system variability. In G. Wefer (Ed.), *The South Atlantic, Present and Past Circulation*, pp. 163–210. Springer-Verlag, New York.

Skogen, M. D. (1999). A biophysical model applied to the Benguela upwelling system. *S. Afr. J. Mar. Sci. 21*, 235–249.

Slowey, N. P. and W. B. Curry (1995). Glacial-interglacial differences in circulation and carbon cycling within the upper western North Atlantic. *Paleonceanography 10*(4), 715–732.

Spero, H. J., J. Bijma, D. W. Lea, and B. E. Bemis (1997). Effect of seawater carbonate concentration on foraminiferal carbon and oxygen isotopes. *Nature 390*, 497–500.

Stephens, C., J. I. Antonov, T. P. Boyer, M. E. Conkright, R. A. Locarnini, T. D. O'Brien, and H. E. Garcia (2002). *World Ocean Atlas 2001, Volume 1: Temperature. S. Levitus, Ed., NOAA Atlas NESDIS 49*. U.S. Gov. Printing Office, Wash., D.C.

Stoll, H. M., D. P. Schrag, and S. C. Clemens (1999). Are seawater Sr/Ca variations preserved in Quaternary foraminifera? *Geochim. Cosmochim. Acta 63*(21), 3535–3547.

Summerhayes, C. P., D. Kroon, A. Rosell-Melé, R. W. Jordan, H.-J. Schrader, R. Hearn, J. Villanueva, J. O. Grimal, and G. Eglinton (1995). Variability in the Benguela Current upwelling system over the past 70,000 years. *Prog. Oceanog. 35*, 207–251.

Tjallingii, R., U. Röhl, M. Kölling, and T. Bickert (2007). Influence of the water content on X-ray fluorescence corescanning measurements in soft marine sediments. *Geochem. Geophys. Geosys. 8*, Q02004, doi:10.1029/2006GC001393.

Tomczak, M. (2000). Seawater density calculator. http://www.es.flinders.edu.au/˜mattom/Utilities/density.html.

Toyofuku, T. and H. Kitazato (2005). Micromapping of Mg/Ca values in cultured specimens of the high-magnesium benthic foraminifera. *Geochem. Geophys. Geosys. 6*(11), Q11P05, doi: 10.1029/2005GC000961.

Toyofuku, T., H. Kitazato, H. Kawahata, M. Tsuchiya, and M. Nohara (2000). Evaluation of Mg/Ca thermometry in foraminifera: Comparison of experimental results and measurements in nature. *Paleoceanography 15*(4), 456–464.

Wefer, G., W.-H. Berger, J. Bijma, and G. Fischer (1999). Clues to Ocean History: a Brief Overview of Proxies. In G. Fischer and G. Wefer (Eds.), *Use of Proxies in Paleoceanography: Examples from the South Atlantic*, pp. 1–68. Springer Verlag Berlin Heidelberg.

Wefer, G. and G. Fischer (1993). Seasonal patterns of vertical particle flux in equatorial and coastal upwelling areas of the eastern Atlantic. *Deep Sea Res., Part I 40(I)*, 1613–1645.

Wilke, I., T. Bickert, and F. J. C. Peeters (2006). The influence of seawater carbonate ion concentration [CO_3^{2-}] on the stable carbon isotope composition of the planktic foraminifera species *Globorotalia inflata*. *Mar. Micropal. 58*, 243–258.

Wolf-Gladrow, D. A., J. Bijma, and R. E. Zeebe (1999). Model simulation of the carbonate chemistry in the microenvironment of symbiont bearing foraminifera. *Mar. Chem. 64*, 181–198.

Wolff, T., B. Grieger, W. Hale, A. Dürkoop, S. Mulitza, J. Pätzold, and G. Wefer (1999). On the reconstruction of paleosalinities. In G. Fischer and G. Wefer (Eds.), *Use of Proxies in Paleoceanography: Examples from the South Atlantic*, pp. 207–228. Springer Verlag Berlin Heidelberg.

Wu, G. and C. Hillaire-Marcel (1995). Application of LP-ICP-MS to benthic foraminifers. *Geochim. Cosmochim. Acta 59*(2), 409–414.

Zabel, M. and cruise participants (2003). *Report and preliminary results of METEOR Cruise M 57/2, Walvis Bay – Walvis Bay, 11.02. – 12.03.2003*. Number 220 in Berichte aus dem Fachbereich Geowissenschaften. Fachbereich Geowissenschaften, Universität Bremen.

Zahn, R., K. Winn, and M. Sarnthein (1986). Benthic foraminiferal $\delta^{13}C$ and accumulation rates of organic carbon: *Uvigerina peregrina* group and *Cibicidoides wuellerstorfi*. *Paleoceanography 1*(1), 27–42.

Zeebe, R. E. (1999). An explanation of the effect of seawater carbonate concentration on foraminiferal oxygen isotopes. *Geochim. Cosmochim. acta 63*(13/14), 2001–2007.

Zeebe, R. E., J. Bijma, and D. A. Wolf-Gladrow (1999). A diffusion-reaction model of carbon isotope fractionation in foraminifera. *Mar. Chem. 64*, 199–227.